uOttawa

L'Université canadienne
Canada's university

FACULTÉ DES ÉTUDES SUPÉRIEURES ET POSTOCTORALES

uOttawa

L'Université canadienne
Canada's university

FACULTY OF GRADUATE AND POSDOCTORAL STUDIES

Maureen Curtin

AUTEUR DE LA THÈSE / AUTHOR OF THESIS

M.Sc. (Biochemistry)

GRADE / DEGREE

Department of Biochemistry

FACULTÉ, ÉCOLE, DÉPARTEMENT / FACULTY, SCHOOL, DEPARTMENT

Understanding the role of Parp-1 in the Atrx^{null} Cortex

TITRE DE LA THÈSE / TITLE OF THESIS

David Picketts

DIRECTEUR (DIRECTRICE) DE LA THÈSE / THESIS SUPERVISOR

CO-DIRECTEUR (CO-DIRECTRICE) DE LA THÈSE / THESIS CO-SUPERVISOR

Lynn Megeney

Fraser Scott

Gary W. Slater

Le Doyen de la Faculté des études supérieures et postdoctorales / Dean of the Faculty of Graduate and Postdoctoral Studies

Understanding the role of Parp-1 in the Atrx^{null} cortex

Maureen Curtin

THESIS

Submitted to the School of Graduate Studies in partial fulfilment
of the requirements for the degree of
Master of Science

University of Ottawa
Ottawa, Ontario, Canada
September 2009

© September 2009, Maureen Curtin

Library and Archives Canada

Published Heritage Branch

395 Wellington Street
Ottawa ON K1A 0N4
Canada

Bibliothèque et Archives Canada

Direction du Patrimoine de l'édition

395, rue Wellington
Ottawa ON K1A 0N4
Canada

Your file Votre référence
ISBN: 978-0-494-65534-4
Our file Notre référence
ISBN: 978-0-494-65534-4

NOTICE:

The author has granted a non-exclusive license allowing Library and Archives Canada to reproduce, publish, archive, preserve, conserve, communicate to the public by telecommunication or on the Internet, loan, distribute and sell theses worldwide, for commercial or non-commercial purposes, in microform, paper, electronic and/or any other formats.

The author retains copyright ownership and moral rights in this thesis. Neither the thesis nor substantial extracts from it may be printed or otherwise reproduced without the author's permission.

AVIS:

L'auteur a accordé une licence non exclusive permettant à la Bibliothèque et Archives Canada de reproduire, publier, archiver, sauvegarder, conserver, transmettre au public par télécommunication ou par l'Internet, prêter, distribuer et vendre des thèses partout dans le monde, à des fins commerciales ou autres, sur support microforme, papier, électronique et/ou autres formats.

L'auteur conserve la propriété du droit d'auteur et des droits moraux qui protège cette thèse. Ni la thèse ni des extraits substantiels de celle-ci ne doivent être imprimés ou autrement reproduits sans son autorisation.

In compliance with the Canadian Privacy Act some supporting forms may have been removed from this thesis.

While these forms may be included in the document page count, their removal does not represent any loss of content from the thesis.

Conformément à la loi canadienne sur la protection de la vie privée, quelques formulaires secondaires ont été enlevés de cette thèse.

Bien que ces formulaires aient inclus dans la pagination, il n'y aura aucun contenu manquant.

Canada

Abstract

ATR-X syndrome (OMIM# 30032) is a form of mental retardation that arises from mutations in the *ATRX* gene in humans. Affected individuals often exhibit severe mental retardation, unique facial dysmorphy, psychomotor impairments and urogential abnormalities. ATRX itself is a SWI/SNF-like chromatin remodeling protein whose role in development is not yet fully understood. To study the role of ATRX in the brain, a conditional forebrain knockout model is used. Reduced forebrain size, impaired development/disorganization of the cortex and enhanced apoptosis of cortical progenitors upon differentiation are observed in this $Atrx^{null}$ model. In this study, we show that the conditional knockout of Atrx in the murine cortex results in the increased activation of Parp-1, most strikingly during early corticogenesis. An increase in DNA damage, as determined by higher levels of γH2AX, is also present during this time. This is consistent with the well-characterized role of Parp-1 activation in response to DNA damage. Furthermore, we demonstrate that there is a severe loss of layer V Er81+ neurons in the $Atrx^{null}$ cortex. Loss of Er81+ neurons is associated with impaired motor skills, which is a common feature of ATR-X patients.

Acknowledgments

I would like to firstly acknowledge Dr. David Picketts for accepting me into his lab. I appreciated his supervisory style of both allowing me to explore my own project's direction and being available whenever I needed advice from a more seasoned scientist. He acted as an excellent academic guide during my studies.

I would also like to thank my thesis advisory committee, Dr. Steffany Bennett and Dr. Jeff Dilworth, for taking the time to provide me with useful feedback about my project.

Furthermore, I would like to recognize the Picketts lab members whose time overlapped with my own: Chelsea Corcoran, Marilyne Delorme, Emma Goodall (my ATRX twin), Mike Huh, Pam Lagali, Chantal Medina, Tina Price-O'Dea, Steve Rennick, Matt Todd, Darren Yip and Olivia Zhang. The lab lunches, gatherings, and activities made for a nice break from the science.

Finally, I would like to thank my parents and Alex for their continual support. In addition to putting up with my whining and meltdowns when things did not go as planned, their confidence in me never wavered.

Table of Contents

List of Figures

List of Tables

Abbreviations

ACF: ATP-dependent chromatin assembly and remodeling factor

ADD: Atypical PHD domain common to ATRX, DNMT3a and DNMT3b

ADP: Adenosine diphosphate

AIF: Apoptosis inducing factor

ATMDS: Alpha thalassemia myelodysplastic syndrome, a preleukemic condition

ATP: Adenosine triphosphate

ATRX: Alpha-thalassemia X-linked mental retardation gene

ATR-X: Alpha-thalassemia X-linked mental retardation syndrome

ATRX: Alpha-thalassemia X-linked mental retardation protein

ATRXt: Truncated alpha-thalassemia X-linked mental retardation protein

$Atrx^{null}$: *Foxg1*-cre;$ATRX^{f/y}$ mouse

BDNF: Brain-derived neurotrophic factor

bHLH: Basic-helix-loop-helix transcription factor

BPTF: Bromodomain PHD finger transcription factor

BrdU: 5-bromo-2-deoxyuridine

BRG1: Brahma-related gene 1

BRM: Brahma

CBP: CREB binding protein

CHD family: Chromodomain/helicase/DNA binding domain family

CHRAC: chromatin assembly complex

CNS: Central nervous system

COFS syndrome: Cerebro-oculo-facio-skeletal syndrome

CREB: cAMP-response element binding protein

DAPI: 4',6-diamidino-2-phenylindole

DIG: Digoxigenin

DNA: Deoxyribonucleic acid

DNMT: DNA methyltransferase

ERCC6: Excision repair cross-complementing rodent repair deficiency

FBS: Fetal bovine serum

FOXG1: Forkhead box G1

H1: Histone H1

H2A: Histone H2a

H2AX: Histone H2a variant X

H2B: Histone H2B

H3: Histone H3

H4: Histone H4

HAT: Histone acetyltransferase

HbH: Hemoglobin H tetramers

HD: Homeodomain

HDAC: Histone deacetylase

HP1: Heterochromatin protein 1

ICC: Immunocytochemistry

IHC: Immunohistochemistry

ISWI: Imitation Switch

MeCP2: MethylCpG-binding protein 2

NURF: Nucleosome remodeling factor

PAR: Poly(ADP-ribose)

PARP-1: Poly(ADP-ribose) polymerase-1

PARG: Poly(ADP-ribose) glycohydrolase

PBS: Phosphate buffered saline

PFA: Paraformaldehyde

PHD: Plant homeo domain

PML: Promyelocytic leukemia protein

PML-NB: Promyelocytic leukemia nuclear bodies

RNA: Ribonucleic acid

SMARCAL1: SWI/SNF-related, matrix-associated, actin-dependent regulator of chromatin, subfamily a-like 1

SMARCB1: SWI/SNF-related, matrix-associated, actin-dependent regulator of chromatin, subfamily B, member 1

SNF2: sucrose non-fermenting 2

XLMR: X linked mental retardation

1.0 Introduction

1.1 Chromatin overview and basic structure

Although the eukaryotic nucleus is less than ten micrometres in diameter, it is able to store all the genetic information required for the survival of the cell. This is no small feat, and in order to physically fit approximately two metres of DNA into each nucleus, it is incorporated into the dynamic structure of chromatin. At its most basic level, chromatin is composed of the nucleosome. Each nucleosome consists of one hundred and forty seven base pairs of DNA wrapped 1.7 times around a histone octamer, containing two each of histones H2A, H2B, H3 and H4. Nucleosomes are connected by linker DNA to which histone H1 binds. These DNA-protein complexes are then further condensed and compacted until the DNA is in the form of the chromosome (Figure 1).

1.2 Chromatin modifications

Chromatin is a dynamic structure, and it can alternate between an open and repressed conformation. The repressed state is referred to as heterochromatin and this prohibits access to the DNA. In its more open conformation it is referred to as euchromatin, and it is in this state that the DNA is accessible (Grewal and Jia, 2007). Therefore it is obvious that in addition to the physical accommodation of DNA that chromatin facilitates, its dynamic structure also provides a means to physically control the access of DNA-binding factors and enzymes to the DNA. In this capacity, chromatin acts as a guardian of DNA in order to ensure proper cellular function. In order to facilitate access when necessary (i.e. for transcriptional and repair machinery), chromatin

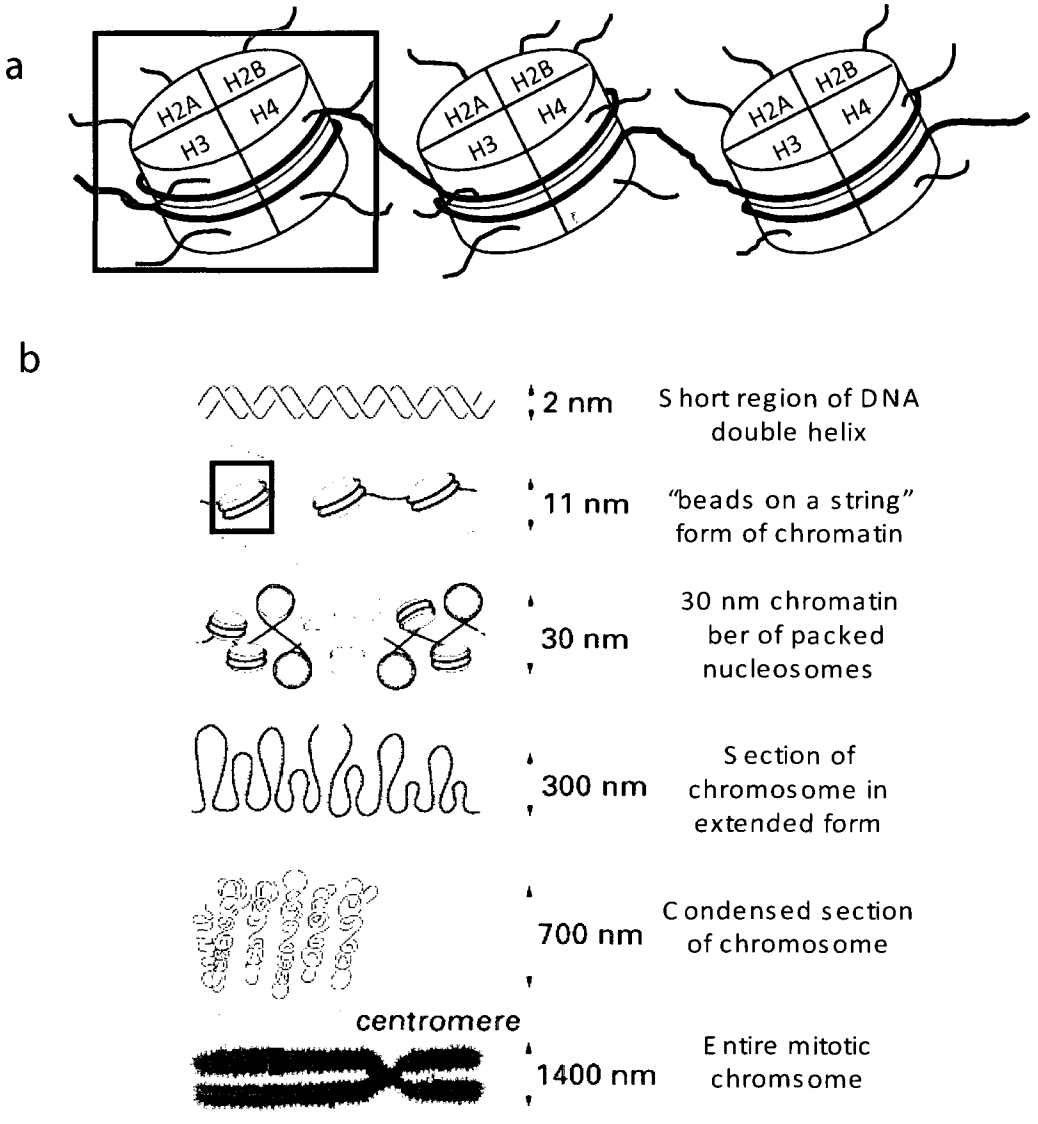

Figure 1: Schematic of the hierarchial packaging of DNA into chromatin.
(a) Each nucleosome consists of one 147 base pairs of double stranded DNA wrapped histone ocatmers to form the 'beads on a string' conformation. Black rectangle is highlighting a single nucleosome. (b) This structure is condensed into the 30 nm chromatin fiber, which is further condensed and compacted until forming the mitotic chromosome. Figure modified from Alberts et al., 2004.

needs to be able to be remodeled—transformed between open and closed conformations. There are three main mechanisms by which to alter chromatin structure: DNA methylation, histone modifications, and ATP-dependent chromatin remodeling (Geiman and Robertson, 2002).

1.2.1 DNA methylation

In mammalian cells, DNA methylation occurs predominantly at CpG islands. Methylation is typically catalyzed by the DNA methyltransferase (DNMT) family of enzymes and results in gene silencing (Geiman and Robertson, 2002; Okano et al., 1998). Additionally, methyl-CpG-binding (MECP) proteins are involved in chromatin remodeling as they bind to modified DNA and recruit chromatin remodeling proteins or regulatory complexes (Meehan et al., 1989). Interestingly, the amount of DNA methylation in humans is higher in the brain than in many other tissues including the liver, spleen, lungs and heart (Ehrlich et al., 1982). DNA methylation is clearly a fundamental process for brain development, as verified by conditional knockout studies of the *DNMT1* gene from neuroblasts. Mice lacking *Dnmt1* do not produce the appropriate methylation patterns of neuronal precursors that are crucial to healthy brain development (Fan et al., 2001).

1.2.2 Covalent Histone Modifications

In addition to the stability that histones ensure for the structure of chromatin, they also have a crucial role in the chromatin remodeling process. The N-terminus of each histone juts out of the nucleosome and is commonly referred to as the histone tail. Like DNA methylation, modifications of histone tails provide epigenetic marks for a particular

chromatin conformation. Specific amino acid residues of histone tails can be modified by a variety of post-translational modifications including methylation, acetylation, phosphorylation, sumoylation, ubiquitination, and ADP-ribosylation. Various modifications (or combinations, thereof) determine gene activity. Some common modifications and their effect on chromatin structure are listed in Table 1. These alterations have the capacity to rework chromatin structure in two distinct ways. Firstly, modifications will change the electrostatic charge of the protein and can thus result in either the compaction or relaxation of chromatin structure. Secondly, certain tail modifications promote the recruitment of non-histone proteins to chromatin (Iizuka and Smith, 2003).

Particularly well-studied are the effects of methylation, acetylation, and phosphorylation. While the methylation of DNA results in a repressive phenotype, the structural outcome of histone methylation is dependent on both the amino acid residue that is targeted and the number of methyl groups that are added (Santos-Rosa et al., 2002). For example, dimethylation of H3K9 is associated with condensed chromatin whereas dimethylation of H3K4 is associated with open chromatin (reviewed by Sharma et al., 2005). The family of proteins that regulate the methylation of histones are known as histone methyl-transferases (HMTs), and specific family members are often required for a specific modification (ex: ASH1 is involved in the modification of H3K4, resulting in active chromatin [Nastase Byrd and Shearn, 2003]). Methylated histone tails regulate several important processes required for proper development including transcription, transcriptional memory, genomic imprinting, and X-inactivation (reviewed in Peters and Schübeler, 2005).

Table 1: Overview of covalent histone tail modifications
Table modified from Kouzarides, T. 2007.

Chromatin Modifications	Residues Modified	Functions Regulated
Acetylation	**K**-ac	Transcription, Repair, Replication, Condensation
Methylation (lysines)	**K**-me1 **K**-me2 **K**-me3	Transcription, Repair
Methylation (arginines)	**R**-me1 **R**-me2a **R**-me2s	Transcription
Phosphorylation	**S**-ph **T**-ph	Transcription, Repair, Condensation
Ubiquitylation	**K**-ub	Transcription, Repair
Sumoylation	**K**-su	Transcription
ADP ribosylation	**E**-ar	Transcription
Deimination	**R > Cit**	Transcription
Proline Isomerization	**P-cis > P-trans**	Transcription

Acetylation status of lysine residues is regulated by histone acetyl transferases (HATs) and histone deacetylases (HDACs). Acetylation decreases the interaction of the positively charged tails with the negatively charged DNA and thus results in relaxation of the nucleosomes and an open chromatin structure. HDACs catalyze the removal of acetyl groups and allow nucleosomes to pack together more tightly to form a condensed form of chromatin (reviewed by Hsieh and Gage, 2005). Another interesting covalent modification is histone phosphorylation. In particular, this modification has an important role in chromatin remodeling following DNA damage. H2AX, a histone variant that comprises between 2-25% of the H2A pool, is rapidly phosphorylated at Ser137 in response to DNA damage. This modification is thought to result in an open chromatin state in addition to acting as a signal to recruit DNA repair proteins to the site of damage (Rogakou et al., 1998; Fernandez-Capetillo et al., 2004).

1.2.3 ATP-dependent chromatin remodeling

Unlike DNA methylation and histone modifications, ATP-dependent chromatin remodeling requires energy derived from ATP hydrolysis to physically disrupt nucleosomes to grant access to the DNA. The histone octamers can slide along the DNA, transfer from one strand of DNA to another, or exit the DNA completely (Johnson et al., 2005). Several categories of ATP-dependent chromatin remodelers have been identified, but the two best characterized families are Switch/Sucrose non-fermenting (SWI/SNF) and Imitation Switch (ISWI).

The SWI/SNF family of chromatin remodelers was first discovered in yeast, but this family is very highly conserved across species. SWI/SNF complexes are quite large

and contain between 8 and 15 subunits (Lall, 2007). A distinguishing feature of this class of proteins is the presence of a bromodomain, required for protein-protein interactions and for the recognition of acetylated lysines (Haynes et al., 1992; Winston and David Allis, 1999). The bromodomain, as well as certain transcription factors, is thought to be necessary for the initial recruitment of SWI/SNF complexes to nucleosomal DNA. Human cells contain multiple SWI/SNF-like chromatin remodeling complexes that contain the ATPase catalytic subunits brahma (BRM) or brahma-related gene 1 (BRG1) at their core. These complexes play an important role in mammalian development, as was first evidenced when the ablation of Brg1 was found to be embryonic lethal (Bultman et al., 2000). Disruption of Brg1 function upsets cell-cycle regulation and differentiation (Lessard et al., 2007). More specifically, a recent study shows that Brg1 binds target genes important for pluripotency and differentiation (Lessard et al., 2007). RNA interference (RNAi) experiments show that decreased Brg1 results in the downregulation of genes related to pluripotency and an upregulation of genes involved in differentiation (Kidder et al., 2009). This suggests that Brg1 has a role in progenitor maintenance and is consistent with previous findings indicating that the deletion of Brg1 from a particular complex in a neural stem cell population results in a reduction of the stem cell pool (Lessard et al., 2007). In terms of chromatin remodeling activity, SWI/SNF complexes are unique from ISWI complexes in the remodeled products they are capable of generating. SWI/SNF complexes can produce nucleosomes with stable DNA loops, they can exchange H2A/H2B dimers between nucleosomes, and they can transfer whole nucleosomes to a new strand of DNA (Narlikar et al., 2002).

ISWI is a diverse family of ATPases that was originally identified in *Drosophila*,

where null mutations were found to be lethal (Deuring et al., 2000). It has since been identified in many other species including humans. ISWI complexes generally contain between 2-4 subunits, making them considerably smaller than SWI/SNF complexes (Johnson et al., 2005). Also, in lieu of a bromodomain, ISWI contains C-terminal SANT and SLIDE domains responsible for DNA and nucleosome tail binding (Aasland et al., 1996; Corona and Tamkun, 2004). ISWI is a component of several chromatin remodeling complexes including nucleosome-remodeling factor (NURF), chromatin assembly complex (CHRAC) and ATP-dependent chromatin assembly and remodeling factor (ACF). There are 2 mammalian homologs, SNF2L and SNF2H, and these show tissue-specific expression patterns. In mice, Snf2h is ubiquitously expressed and its global deletion results in embryonic lethality (Lazzaro et al., 2001; Stopka and Skoultchi, 2003). Alternately, mouse Snf2l is restricted to the brain and gonadal tissue, suggesting a role for Snf2L in neuronal pathways (Lazzaro et al., 2001; Barak et al., 2004). This idea is supported by the fact that Snf2L is known to be a member of the Nurf complex which regulates the expression of *Engrailed*—a gene implicated in brain development (Barak et al., 2003). Additionally, Snf2l also forms a chromatin remodeling complex with Cecr2, a protein required for neurulation (Banting et al., 2005). More recent work in our lab has shown that Snf2L^{null} mice are viable but have larger brains resulting from hypercellularity, suggesting a role for the protein in cell cycle regulation (Picketts, unpublished). Human SNF2L is known to differ from the mouse homolog in that human SNF2L is ubiquitously expressed. However, its regulation is instead controlled by tissue-specific alternatively spliced isoforms (Barak et al., 2004). The expression of the active form SNF2L is limited to the brain and skeletal muscle, and so the importance of SNF2L

as a regulator of brain development in humans is still likely. The seeming importance of ISWI in development is consistent with previous studies performed in *Drosophila*, where null mutations were found to affect cell viability, cause changes in chromatin structure, and affect gene expression during development (Deuring et al., 2000). Regarding chromatin remodeling activity, a common property of ISWI complexes is their ability to regulate spacing of intact nucleosomes, something SWI/SNF members are not capable of. Since ISWI and SWI/SNF have different chromatin remodeling capabilities, it is likely that their roles in the cell are also distinct (Narlikar et al., 2002).

1.3 Chromatin remodeling and disease

Chromatin remodeling is clearly important for the life of a cell, as it is necessary for the organization of the genome to ultimately help to control gene transcription, replication, recombination and repair. In view of the fact that chromatin remodeling is fundamental for healthy cellular function, it is no surprise that disruption of chromatin remodeling proteins leads to various human diseases. A list of chromatin remodeling proteins and the diseases associated with their mutations is shown in Table 2.

Since SWI/SNF complexes have been implicated in cell-cycle regulation, it stands to reason that deficiencies or misexpression of some of these chromatin remodelers result in cancer. Altered expression of the proteins BRG1, BRM, and SWI/SNF-related, matrix-associated, actin-dependent regulator of chromatin, subfamily B, member 1 (SMARCB1) has been identified in a variety of tumor cell lines (Betz et al., 2002; Huang et al., 2003). While the aforementioned proteins all exhibit ATP-dependent mechanisms of activity, cancer can also result from misregulation of other types of chromatin

Table 2. A summary of epigenetic regulators and the associated human diseases resulting from their deficiency. Table modified from Higgs et al., 2007.

Nonhistone chromatin protein	Example	Disease
DNA methyltransferases	DNMT1, DNMT3A, DNMT3B	ICF Syndrome (DNMT3B)
Methyl-binding proteins	MBD1-4, MeCP2 Kaiso	Rett Syndrome (MeCP2)
Histone acetyltransferases	CBP, p300	Rubenstein-Taybi Syndrome (CBP, p300)
Histone methyltransferases	Suv39H1/2, EzH2	Sotos Syndrome (NSD1)
Histone kinase	RSK2	Coffin-Lowry Syndrome (RSK2)
Histone demethylases	LSD1, JHDM1	
Chromatin remodeling proteins	BRG, BRM, CHD1-9, ATRX	Schimke Immunosseous Dysplasia (SMARCAL1) Cockayne Syndrome (ERCC6) ATRX Syndrome (ATRX) CHARGE Syndrome (CHD7)
Histone binding	Hp1α,β,γ	
Polycomb group proteins	Pc,Suz12	

remodelers. Mutations in certain proteins with HAT activity including cAMP-response element binding protein (CREB) binding protein (CBP), E1A binding protein 300 (EP300), and ZNF220 also cause cancer (Gayther et al., 2000; Kung et al., 2000; Sugita et al., 2000).

Cancer is not the only aberrant phenotype resulting from improper chromatin remodeling. Mutations in the SWI/SNF related, matrix associated, actin dependent regulator of chromatin, subfamily a-like 1 (SMARCAL1) protein results in Schimke immuno-osseus dysplasia. Individuals with this disease have a weakened immune system due to a shortage of T-cells as well as kidney problems and bone-marrow failure (Boerkoel et al., 2002). Furthermore, a role for chromatin remodeling has been elucidated in noncoding repeat expansion diseases such as Fragile X syndrome, wherein the repeats are able to induce heterochromatin formation (Kumari and Usdin, 2009).

Finally, a common result of misfunctioning chromatin remodeling proteins is some degree of mental retardation, often accompanying other physical ailments. Mutations in excision repair cross-complementing rodent repair deficiency, complementation group 6 (ERCC6), a SWI/SNF related ATPase involved in DNA repair, results in both cerebro-oculo-facio-skeletal (COFS) syndrome and Cockayne syndrome (type B) (Huang et al., 2003; Van Hoffen et al., 1993). Also, in addition to the cancer stated earlier, CBP mutations can result in Rubinstein Taybi syndrome, a type of mental retardation accompanied by facial anomalies, broad digits and short stature (Murata et al., 2001). Another example is found in females who are heterozygous for mutated MeCP2, a protein involved in DNA methylation, who have a severe form of mental retardation known as Rett syndrome (Amir et al., 1999; Sung Jae Lee et al., 2001).

1.4 X-Linked Mental Retardation

Mental retardation is a serious condition that has been estimated to affect between 1-3% of the Western population (Leonard and Wen, 2002). It is clinically defined by the Journal of Medical Genetics as follows:

> "[For an individual to be considered mentally retarded] there must be significant sub-average general intellectual functioning accompanied by limitations in adaptive functioning in at least two of the following skill areas: communication, self care, home living, social/interpersonal skills, use of community resources, self-direction, functional academic skills, work, leisure, health, and safety (criterion B). The onset must also occur before 18 years of age (criterion C) (Raymond, 2006)."

Since the early 20th century, it has been noted that a higher proportion of mental retardation cases are found in males as compared to females. This is due to the fact that mutations of more than 80 different genes found on the X chromosome result in some form of mental retardation (Chiurazzi et al., 2008). To date, over 200 types of X-linked mental retardation disorders have been described (Lisik and Sieron, 2008). The distribution of the genes causing X-linked mental retardation are shown in Figure 2, but of particular interest to this project is the *ATRX* gene, cause of the ATR-X syndrome.

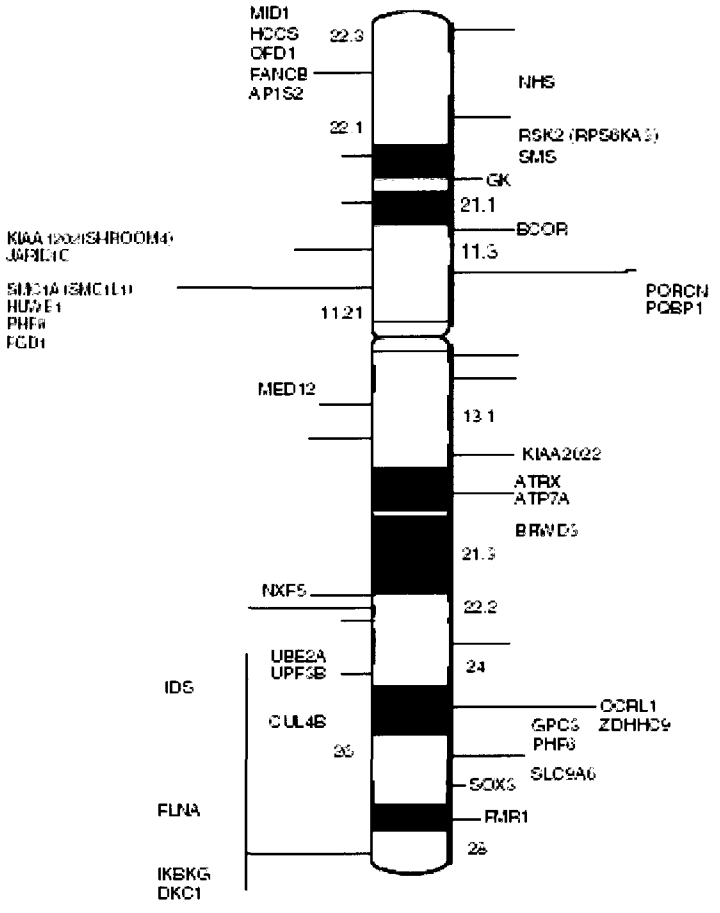

Figure 2: Distribution of genes along the X chromosome known to be associated with X-linked mental retardation.
The position of the 82 known XLMR genes on the X chromosome. Genes in black are known to cause syndromes, genes in grey with an asterisk are nonspecific mental retardation genes and genes in grey with a + sign are involved in neuromuscular disorders. Figure taken from Chiurazzi, P. et al., 2007.

1.5 ATRX

1.5.1 Clinical features of the ATR-X Syndrome

Alpha thalassemia mental retardation, X-linked (ATR-X) syndrome (OMIM #30032) is a type of X-linked mental retardation that results from mutations in the *ATRX* gene. It is very rare and its prevalence has been estimated at < 1-9/1 000 000 (Gibbons, 2006). As of 2008, over 200 individuals were confirmed to have ATR-X syndrome, and it resulted from any of the 113 identified mutations (Gibbons et al., 2008). Additionally, ATR-X syndrome in 2 patients resulted from a partial intragenic duplication of *ATRX* that resulted in loss of function of the protein (Thienpont et al., 2007). ATR-X syndrome can be identified clinically by a multitude of common physical manifestations. In 90% of cases there is a unique facial dysmorphy which includes wide-set eyes, a broad upturned nose, a tented upper lip and an everted lower lip (Figure 3) (Gibbons, 2006). Additionally, 80% of individuals have some form of urogenital abnormalities ranging from mild problems such as undescended testes to the most severely affected individuals who exhibit male pseudohermaphrodism (Gibbons, 2006; Ion et al., 1996; McPherson et al., 1995). Importantly, 90% of individuals also have some degree of alpha thalassaemia, which is a type of anemia whereby the alpha portion of hemoglobin is not properly produced. Instead, excess beta chains are produced and form tetramers known as Hemoglobin H (HbH) inclusions. Alpha thalassemia can be diagnosed by incubating venous blood with 1% cresyl blue in isotonic solution and then searching for HbH inclusions by microscopy (Gibbons, 2006). However, it is important to note that HbH inclusions only appear after alpha globin is reduced by at least 50%, so less severe cases

Figure 3: Two unrelated children presenting with common dysmorphic facial features associated with ATR-X syndrome
Two ATRX patients presenting with the characteristic facial features including upswept frontal hair line, hypertelorism, epicanthic folds, flat nasal bridge, small triangular upturned nose, tented upper lip, everted lower lip and hypotonic facies. Figure modified from Gibbons, RJ, 2006.

of alpha thalaessemia cannot be diagnosed by this process. Other common effects of ATR-X syndrome include microcephaly in 75% of patients, skeletal abnormalities in 90% of patients, and a variety of other features including psychomotor impairment, short stature, seizures, cardiac defects, and kidney problems (Gibbons, 2006).

While there has not yet been a comprehensive behavioural study completed for patients with ATR-X syndrome, certain mannerisms have been noted by doctors and caregivers. Firstly, individuals with ATR-X syndrome have been described by their parents or caregivers as being generally content. However, there are reports of largely fluctuating emotions between, for example, excitement and depression. It is likely that some of the sudden onset periods of negative outbursts are associated with pain from the symptoms of ATR-X syndrome. There is a wide spectrum of other behavioural phenotypes that have been observed in affected individuals including autistic-like behaviour, self-injury, restlessness, or obsessive behaviour (Gibbons, 2006; Wada et al., 1998).

Since ATR-X syndrome is X-linked, carrier females do not exhibit observable effects of the syndrome. Screens show that carriers exhibit skewed X inactivation so as to preferentially inactivate the X chromosome containing mutations in *ATRX* (Wada et al., 2005). Although carriers are not obviously affected intellectually, 25% show signs of subtle alpha thalassemia (Gibbons, 2006). Interestingly, a single case of a female affected with ATR-X syndrome was identified, but analysis showed a complete skewing of the inactivated X towards the chromosome containing the non-mutated *ATRX* gene (Badens et al., 2006).

In addition to the constitutional mutations of *ATRX* that result in ATR-X syndrome, acquired mutations of *ATRX* at a later stage of life are found in individuals with alpha thalassemia myelodysplastic syndrome (ATMDS). ATMDS is a preleukemic condition that occurs mainly in older men. In general, the alpha thalassemia exhibited in ATMDS patients is much more severe than ATRX patients. For example, a boy with ATR-X syndrome had only 0.1% HbH, while a man whose ATMDS was caused by the exact same mutation had 50% HbH (Gibbons et al., 2008). The reason for this large difference is unknown.

1.5.2 Molecular genetics of the ATR-X syndrome

The *ATRX* gene is located on the X chromosome at Xq13. It contains 35 exons whose transcription and translation results in the synthesis of a 280 kDa protein (Figure 4). At its N-terminal region, *ATRX* contains an ATRX-DNMT3-DNMT3L (ADD) domain, which is a plant homeo domain (PHD) -like zinc finger with an additional C2-C2 motif. This domain is so far known to be unique to the *ATRX*, *DNMT3* and *DNMT3L* genes. PHD zinc fingers have been traditionally found in many chromatin-associated proteins and often facilitate protein-protein interactions (reviewed in Bienz, 2006). Interestingly, mutations in the PHD of several proteins are associated with a variety of human pathologies including immunological disorders, cancer, and mental retardation (Baker et al., 2008). At its C-terminal end, ATRX contains seven helicase motifs and an ATPase domain of the SNF2 family. It is this domain that is the catalytic powerhouse of the protein, and the SNF2 domain is suggestive of ATRX having chromatin remodeling activity. However, the definitive cellular role of ATRX is likely complex and is not yet fully understood. In addition to the full-length ATRX protein, a truncated form of ATRX

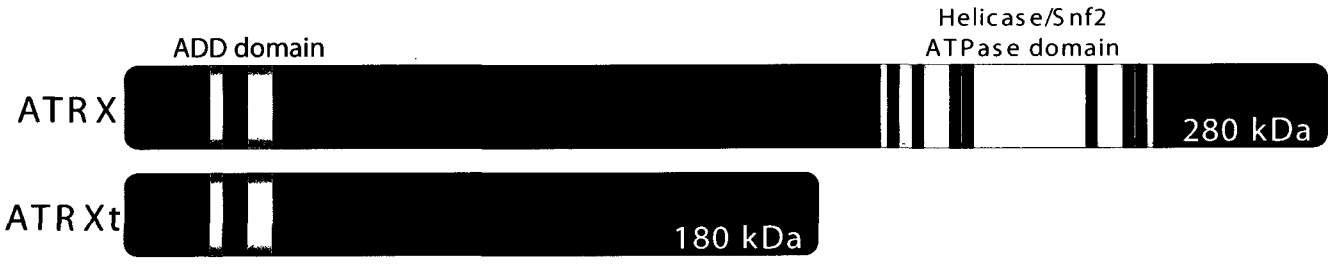

Figure 4: Schematic of the *ATRX* gene
Diagram of the *ATRX* gene. Alternative splicing produces two possible ATRX proteins. The 280 kDa full-length protein contains an N-terminal ADD domain and a C-terminal SNF2 helicase domain. The truncated 180 kDa isoform only contains the ADD domain. Figure modified from Gibbons, RJ, 2008.

(ATRXt) results from the transcription of only the first 11 exons. ATRXt contains the ADD domain but not the ATPase domain. Mutations that affect both ATRX and ATRXt are not more severe than ATRX alone, likely due to the fact that ATRXt is lacking the enzymatic abilities of the ATPase domain (Garrick et al., 2004).

From a molecular perspective, ATR-X syndrome arises from mutations in the *ATRX* gene. While it is known that most mutations leading to the ATR-X syndrome are missense mutations, for a long time there were no obvious genotype:phenotype correlations. However, a 2008 study confirmed that 50% of mutations are clustered in the ADD domain and affected individuals with mutations in this area show severe psychomotor impairment (Badens et al., 2006; Gibbons et al., 2008). Furthermore, mutations in the region of the gene that is C-terminal to the helicase domain have been associated with severely impaired urogenital development (Gibbons et al., 2008).

1.5.3 Localization and function of ATRX protein

While the exact function of ATRX remains unknown, the 280 kDa protein has been shown to have not only an important role in many cellular processes, but its function can be dependent on its localization. Early studies of the protein showed that ATRX localizes to pericentromeric heterochromatin during mitosis and interphase via its PHD zinc fingers and its association with heterochromatin protein 1 (HP1) (McDowell et al., 1999; Bérubé et al., 2000). This is easily detectable by immunofluorescent staining as ATRX co-stains with DAPI bright spots. Additionally, ATRX has been shown to interact with the methyl-CpG-binding protein MeCP2. This interaction has been confirmed both *in vitro* and *in vivo* and it has been shown to be disrupted in *in vitro* models of Rett

syndrome (Nan et al., 2007). Furthermore, ATRX localization is misplaced from heterochromatin in the *Mecp2*^{null} brain. This mislocalization is not a result of a breakdown in heterochromatin integrity as DAPI staining remained intact. Since mutations in both of these proteins are known to contribute to mental retardation, it is possible that the maintenance of the interaction is necessary for normal brain function (Nan et al., 2007).

In 2003, progress was made in the ATRX field when Xue et al. were able to isolate ATRX in its protein complex, a previously unattainable feat. It was found that ATRX associates in complex with the transcription cofactor death domain-associated protein (Daxx), and that this complex localizes to promyelocytic leukemia (PML) nuclear bodies. ATRX is recruited to PML bodies by Daxx, which it binds to via amino acids 1189-1326 (Tang et al., 2004). Additional study of the ATRX/Daxx complex further supported the idea that ATRX had chromatin remodeling capabilities, as the complex showed common chromatin remodeling tendencies including triple-helix displacement activity and the ability to alter nucleosome DNase I digestion patterns; both activities dependent on ATP (Xue et al., 2003).

In addition to the likelihood that ATRX is an ATP-dependent chromatin remodeling protein, several studies suggest that ATRX also plays a role in gene expression by regulating certain methylation patterns. For example, a study of metaphase preparations showed that ATRX consistently binds to the short arms of acrocentric chromosomes—an area of the genome that contains a high proportion of ribosomal DNA (rDNA) (McDowell et al., 1999). In individuals with the ATR-X syndrome, while the localization of ATRX to this area remains intact, rDNA is found to be hypomethylated as

compared to unaffected individuals (Gibbons et al., 2000). Further methylation abnormalities were found in both a repeating element of the Y chromosome and subtelomeric repeats. This effect of ATRX on methylation can likely be attributed to the homology of its ADD domain with the DNMT3 family of methyltransferases. These classic chromatin remodeling properties of DNA methylation suggest a likely mechanism of ATRX involvement in gene silencing (Gibbons et al., 2000). Further evidence for this functional property of ATRX was supplied in 2009, when a study implicated ATRX in the process of X chromosome inactivation. Using embryonic fibroblasts and primary ovarian granulosa cell lines, FISH experiments showed that ATRX preferentially gathers on the inactive X chromosome (Xi) in female somatic cells. Its association with Xi is stable, and the persistence of its localization through mitosis and differentiation are suggestive of a role for ATRX in the maintenance of the inactivated X chromosome. ATRX is not believed to be necessary for the initiation of X chromosome inactivation (Baumann and De La Fuente, 2009).

In addition to its general implication in epigenetic gene regulation, several studies have implicated ATRX in the regulation of the cell cycle. Firstly, the localization of ATRX is altered based on the stage of the cell cycle. *In vitro* studies using Hela cells showed that ATRX associates with the core nuclear matrix—a protein-RNA structure within the cell's nucleus. This association occurs at interphase, at a point in the cell cycle when ATRX is hypophosphorylated. However, upon initiation of mitosis, ATRX localization shifts from the nuclear matrix to condensed chromatin. This shift occurs in conjunction with the phosphorylation of ATRX (principally at serine residues) and its association with HP1α (Bérubé et al., 2000). In addition to proper localization, proper

function of ATRX is also necessary for an operational cell cycle. Throughout meiosis of mammalian oocytes, functional ATRX in conjunction with standard meiotic epigenetic modifications is necessary for proper chromosomal alignment at the metaphase plate during metaphase II (De La Fuente et al., 2004). A more recent study also implicates ATRX in proper chromosome alignment, as cultured human cells and neuroprogenitors lacking ATRX were shown to experience a slower transition from prometaphase to metaphase. This prolonged cell division process manifested as impaired chromosome congression at the metaphase plate and reduced cohesion between sister chromatids, as evidenced by increased distance between their kinetochores (Ritchie et al., 2008).

While the above findings mostly focus on the role of ATRX in the brain and the cell cycle, ATRX has also been shown to play a role in sex differentiation. This is consistent with the fact that urogenital abnormalities are associated with the ATR-X syndrome resulting from mutations in the human gene. While its exact role in sex differentiation is unclear, the underdeveloped genitalia and testicular dysgenesis that has been observed in some patients suggests that ATRX is required early during sex differentiation (Tang et al., 2004).

1.6 Mouse Models of the ATR-X syndrome

In order to better study the human ATR-X syndrome, an important step in the progression of research was the development of a mouse model. Initially, *Atrx* was inactivated at the 8- to 16-cell stage of development. It was determined that embryos lacking Atrx were able to normally implant and gastrulate but eventually died around E9.5 due to malformation of the embryonic trophoblast. This study showed the necessity

of Atrx for the proper development of the murine trophoblast and that a global deletion of Atrx was thus embryonic lethal (Garrick et al., 2006).

In 2002, Bérubé et al. developed a transgenic mouse that overexpresses ATRX. At embryonic stages, transgenic mice exhibited neural tube defects, neuroepithelial defects, retarded growth, and misorganization of the ventricular zone. While there was a high incidence of embryonic lethality, those embryos that did survive until birth had high incidences of seizures, craniofacial abnormalities, and perinatal death. In summary, mice that overexpress a human ATRX protein show neurodevelopmental abnormalities, suggesting that ATRX is necessary for proper brain development (Bérubé et al., 2002).

In light of what was learned from the transgenic model, the next step was to develop a conditional forebrain knockout of ATRX. A cre/lox system was employed to conditionally knock out Exon 18 of *Atrx*, resulting in the ablation of the full-length ATRX protein. ATRXt is still produced. While knockout embryos do survive until birth, they are smaller than their wildtype littermates and die within the first few days postnatally due to dehydration (Figure 5). Additional phenotypic effects include a reduction in forebrain size resulting from widespread hypocellularity of the cortex and hippocampus. The dentate gyrus is also lacking. A combination of neuronal birthdating experiments and TUNEL staining at a variety of embryonic time points showed that this loss of cortical mass in knockout embryos was due to increased apoptosis rather than defective proliferation (Bérubé et al., 2005). More recently, it has been shown that the observed apoptosis is occurring via the intrinsic pathway (Picketts, unpublished) and is mediated by the tumor suppressor protein, p53 (Seah et al., 2008).

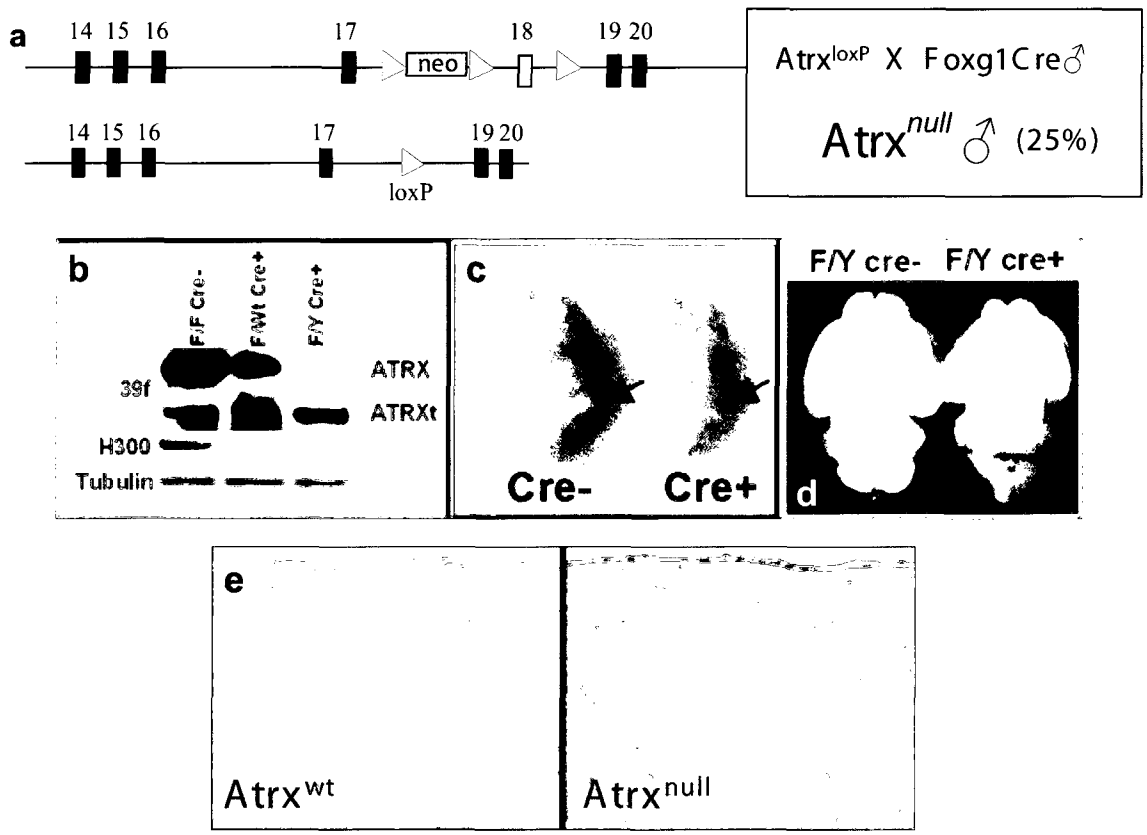

Figure 5: Conditional forebrain knockout of Atrx gene
(A) Matings between Atrx$^{flox/flox}$ females and Foxg1-cre$^{+/-}$ males employs the use of a cre/lox system to excise Exon 18, resulting in 25% of offspring lacking Atrx in the forebrain. **(B)** Western blot confirms the loss of the full length ATRX protein. ATRXt remains. **(C)** Postnatal Atrx^{null} mice are smaller than their wildtype littermates. Arrow is highlighting the lack of milk in the belly of the Atrx^{null} pup. **(D)** Forebrain size is reduced in the Atrx^{null} mice. **(E)** Cortical hypocellularity was demonstrated in Atrx^{null} forebrains and was attributed to a 12-fold increase in apoptotic cells at E11.5. Figure modified from Bérubé et al, 2005.

1.7 Development of the mouse neocortex

To understand the role of ATRX in neuronal development, it is first essential to garner a basic understanding of corticogenesis. The brain is divided into three main areas: The forebrain, the midbrain, and the hindbrain. The forebrain, which is of most interest to this project, contains the hippocampus and the cortex. The neocortex is the most recently evolved part of the cortex and it is comprised of six layers (Figure 6). Mouse neocortical development occurs from E11.5 to E18.5, with layers developing in a very specific manner. At E11.5, the cortex consists predominantly of progenitor cells situated in a layer known as the ventricular zone (VZ). The first wave of post-mitotic neurons migrates radially to form the preplate (PP). At E12.5-13.5, the PP is split by a second wave of neurons migrating away from the VZ. These neurons form the cortical plate, sandwiched in between what is then known as the superficial marginal zone and the subplate (SP). Between E14.5 and E18.5, neurons continue to depart the VZ in waves and migrate outwardly to continue to thicken the cortical plate (CP). The layers form in an inside-out manner, with the later-born neurons continuing to migrate past earlier born neurons before settling closer to the skull. Once the CP is fully formed with six layers, the SP degrades. Each layer can be characterized by certain molecular markers expressed, and the neurons of various layers have certain distinct functions (Gupta et al., 2002).

1.8 Poly(ADP-ribose) Polymerase-1

Much of the work presented in this thesis explores the role of PARP-1 activation in the cortex of mice lacking Atrx. As such, here we present information of this protein.

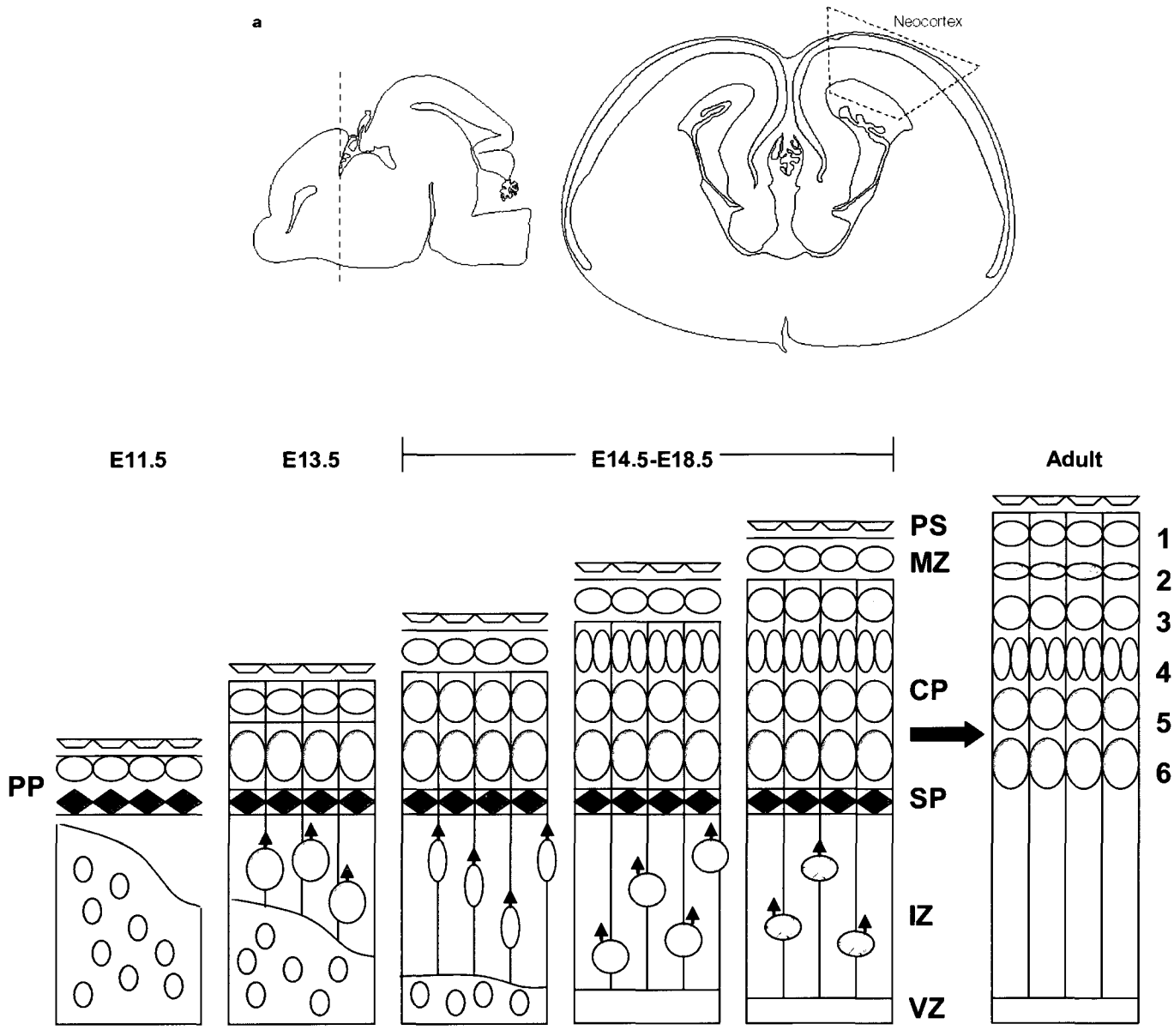

Figure 6: Development of the mouse neocortex
(A) The location of the neocortex in the central nervous system. A lateral view of an E16.5 mouse brain (left). The red dashed line indicates the plane of section from which a coronal section (right) has been taken, which shows the location of the neocortex. **(B)** A schematic of cortical development occurring between E11.5 and E18.5, eventually forming the 6-layered adult neocortex. *PP: preplate; VZ: ventricular zone; IZ: intermediate zone; SP: subplate; CP: cortical plate; MZ: marginal zone; PS: pial surface.* Figure modified from Gupta et al. 2002.

The poly(ADP-ribose) polymerase (PARP) family of enzymes was first discovered in 1963 (Chambon et al., 1963). PARP-1 is the most abundant and most well-characterized member of the PARP family, with each nucleus containing between 1 and 2 million copies of the enzyme. PARP-1 is a 113 kDa nuclear enzyme that catalyzes the posttranslational modification of poly(ADP-ribosyl)ation (PARylation) (Figure 7). PARP-1 uses the coenzyme nicotinamide adenine dinucleotide (NAD+) as a substrate to transfer ADP-ribose units to acceptor proteins while releasing nicotinamide as a by-product. PAR chains can extend up to 200 units in length and additionally, can branch off to further extend the modification. The other side of PARP metabolism involves poly(ADP-ribose) glycohydrolase (PARG) which cleaves PAR into single ADP-ribose units (D'Amours et al., 1999).

The *PARP-1* gene contains 3 domains: The N-terminal DNA-binding domain (DBD), the central automodification domain (AMD), and the C-terminal catalytic domain. The DBD contains two zinc fingers that bind to altered structures in DNA (i.e. breaks) as well as two helix-turn-helix motifs that mediate strong interaction with DNA. The AMD is the site that is poly(ADP-ribosyl)ated, and it also contains a BRCT domain that allows for certain protein-protein interactions. The catalytic domain catalyzes the initiation, elongation, and branching of PAR polymers, and it also contains the "PARP signature" found in all PARP family members (Figure 8) (Kraus and Lis, 2003).

While PARP-1 is known to have a role in many cellular processes including chromatin remodeling, DNA replication, transcription, apoptosis, and inflammatory response, its most well-characterized role is in DNA damage and repair. When DNA is damaged, PARP-1 is recruited to the site of the break. This activates its enzymatic

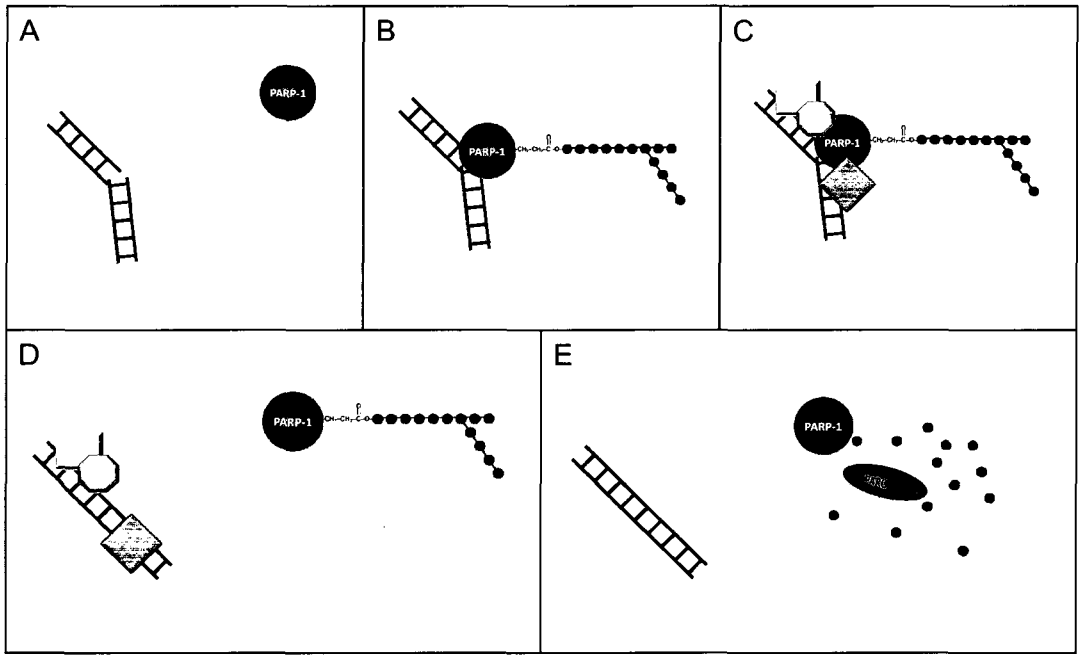

Figure 7: PARP-1 metabolism
(A) PARP-1 is recruited to breaks in DNA; **(B)** PARP-1 binds to the break and automodifies by adding units of poly(ADP-ribose) to its automodification domain; **(C)** DNA repair proteins are recruited to the site of damage; **(D)** automodified PARP-1 is released from the repairing DNA; **(E)** PARG breaks up long chains of poly(ADP-ribose), resulting in naked PARP-1 and mono ADP-ribose units in the cell.

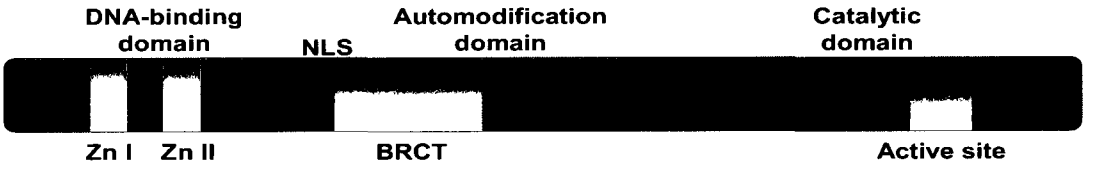

Figure 8: *PARP-1* gene
The *PARP-1* gene contains 3 domains: The N-terminal DNA-binding domain (DBD), the central automodification domain (AMD), and the C-terminal catalytic domain. The DBD contains 2 zinc fingers. The AMD contains a nuclear localization signal (NLS) and a BRCT interaction site. The catalytic domain contains an active site, responsible for the protein's activity.

activity and it begins to automodify with the addition of PAR units. This PAR extension acts as a signal to recruit DNA repair proteins to the site of the break. PARP-1 is therefore vital in the normal initiation of the DNA damage response. This claim was further supported by the generation of a Parp-1 knockout (KO) mouse, as it exhibits impaired DNA damage repair (Wang et al., 1995; Ménissier-de Murcia et al., 1997; Masutani et al., 1999).

1.8.1 PARP-1 and chromatin

As mentioned above, PARP-1 plays a role in the regulation of chromatin structure. Depending on the physiological environment, PARylation will cause either the compaction or decompaction of chromatin (Tulin et al., 2002; Tulin and Spradling, 2003; Tulin et al., 2003). Studies have also shown that both automodified and non-modified PARP-1 associates with histones. *In vitro,* PARP-1 associates with H2A and H2B, while a PARP-1 association with H1 in *Drosophila* causes the protein's release from chromatin (Kim et al., 2004).

Additionally, PAR modifications can act as docking stations for chromatin modifiers. For example, DNMT1 binds to the automodification of PARP-1, is subsequently PARylated as well, and its own methyltransferase activity is then inhibited ((Reale et al., 2005)Quénet et al., 2009). Moreover, some DNA repair proteins containing zinc fingers have been found to bind PARylated proteins via these domains, comparable to the way that bromodomains recognize acetylation (Ahel et al., 2008). Although the ATRX protein contains PHD zinc fingers, no interaction between ATRX and PARP-1 has been elucidated as of yet.

PARP-1 also has a role in dictating the general chromatin environment of the nucleus—i.e. heterochromatin versus euchromatin. In 2007, Nusinow et al. showed that upon association with the histone variant macroH2A1.2, PARP-1 activity is arrested and this contributes to the silencing of the inactivated X chromosome (Nusinow et al., 2007). PARP-1 and other PARP family members are also known to associate with several centromeric proteins and together these interactions maintain pericentromeric heterochromatin (Saxena et al., 2002a; Saxena et al., 2002b).

1.8.2 PARP-1 in neuronal death pathways

Since PARP-1 is involved in so many cellular processes, it is no surprise that it is implicated in cell death pathways. However, its role is multi-faceted. For example, during caspase-mediated apoptosis, PARP-1 is cleaved by caspase-3 into a 24 kDa and an 89 kDa fragment (Kaufmann et al., 1993). The remaining fragments are non-functional. It is hypothesized that this cleavage occurs to assure that apoptosis is not hindered by attempts to repair DNA breaks. If cleavage does not occur, excessive breaks could lead to the depletion of cellular stores of NAD+. The oxido-reduction capacity of NAD+ is vital in the generation of ATP, the cell's major source of energy. Therefore depletion of NAD+ can lead to cessation of energy-dependent cell function and thus eventually necrotic death (Shiao Li Oei and Ziegler, 2000; Chiarugi, 2002).

Interestingly, PARP-1 has also more recently been shown to have a central role in caspase-independent apoptosis. PARP-1 activates in response to genotoxic stress, and its automodification leads to the translocation of apoptosis inducing factor (AIF) from the mitochondria to the nucleus (Yu et al., 2002; Yu et al., 2003). This allows AIF to induce

apoptosis without any reliance on the caspases. The exact mechanism by which PARylation regulates AIF is unknown, but it is hypothesized that PARP-1 automodification somehow acts as a signal for the release of AIF.

PARP-1 also has a secondary role in neurotoxicity. The activation of N-methyl-D-aspartate (NMDA) receptors can result in neuronal damage due to an influx of intracellular calcium. This influx activates a variety of enzymes including proteases, endonucleases, phospholipases, and nitric oxide synthase (NOS). The resulting production of NO by NOS results in the formation of peroxynitrite, which is an anion that can form free radicals and become a DNA damaging agent (Koh et al., 2005b; Koh et al., 2005a). This damage eventually stimulates PARP-1 activity. This pathway of PARP-1 activation is known to occur in conditions of stroke, ischemia, and certain neurodegenerative diseases including Parkinson's disease.

1.9 Rationale and Research Objectives

In the last several decades, research has shown that epigenetic control of gene regulation is a huge factor in human health and disease. Particularly interesting is the idea that epigenetic regulation of chromatin dynamics is key in maintaining a healthy cell. If this control is compromised, the resulting misregulation of chromatin dynamics can result in disease. The ATR-X syndrome, caused by mutations in the chromatin remodeling gene *ATRX*, is one such example.

The conditional knockout of Atrx in the forebrain leads to obvious phenotypic consequences including hypocellularity resulting from increased apoptosis of neuronal precursors. Since ATRX is a known interaction partner of Daxx, a facilitator of extrinsic

apoptosis, and a knockdown study of Daxx showed cleavage of PARP-1, PARP-1 was a logical player to further examine. Surprisingly, initial examination of Parp-1 did not show its cleavage in the Atrx^{null} cortex, but was instead found in increased levels. This finding, in addition to the fact that PARP-1 is known to be involved in neuronal death pathways, led us to **hypothesize that increased Parp-1 activity either enhances the cell death observed in Atrx^{null} mice or promotes the survival of neurons in this model.**

To address this hypothesis, we focused on three specific aims:

1. Characterizing the expression of Parp-1 in corticogenesis;
2. Examining the *in vivo* expression patterns of Parp-1 in Atrx^{null} mice;
3. Determining the mechanism of Parp-1 involvement in Atrx^{null} phenotype.

2.0 Materials and Methods

2.1 General Materials

All plasticware including cell culture dishes, 15 ml and 50 ml tubes, and microcentrifuge tubes were obtained from Fisher Scientific (Ottawa, ON). Disposable pipettes and gloves were obtained from VWR (Mississauga, ON), while micropipettes were obtained from Gilson (Guelph, ON). Commonly used reagents including agarose, EDTA, ethidium bromide, Glycine, KCl, KH_2PO_4, NaCl, Na_2PO_4, NaCl, KCl, SDS, TRIS, Tween-20 and Triton-X were obtained from Fisher Scientific (Ottawa, ON), Sigma-Aldrich (Oakville, ON), and Invitrogen (Burlington, ON). Ethanol, methanol and sterile HPLC water were obtained from Fisher Scientific (Ottawa, ON). The specific supplier information for other materials used is listed throughout the methods section.

2.2 Mouse Neuroblastoma N1E115 cultures

N1E115 cells were obtained at a low passage number and maintained in a growth phase in 7-8 ml of proliferation media (10% FBS, 1% penicillin/streptomycin in DMEM) in a 10 cm petri dish. All cultures were incubated at 37°C with 5% CO_2. Cultures of at least 80% viability (based on adherence) were either split into multiple dishes or used for experimental purposes upon reaching 80% confluency. To induce differentiation, proliferation media was aspirated and was replaced with 7-8 ml of differentiation media (1% FBS, 1% penicillin/streptomycin, 1% DMSO in DMEM). To obtain cells for a differentiation time course, 2 dishes of cells were harvested from each 24 hour time point beginning at Day 0 (i.e. growth) and ending at Day 7 of differentiation. To obtain the cell

pellets, differentiation media was aspirated and replaced with 3 ml of Trypsin for 5 minutes at 37°C. Cells were then sloughed off plates with 7 ml of sterile 1X phosphate buffered saline (PBS) and centrifuged at 1 000 rpm in a table top Heraeus Instruments Megafuge 1.0 for 5 minutes. 1X PBS/trypsin was then aspirated and the pellet was washed once more in PBS. PBS was removed and the pellet was then stored at -80°C until needed.

2.3 Animal Husbandry and Tissue Preparation

2.3.1 Generation of $Atrx^{null}$ embryos

In order to attain the conditional forebrain ATRX knockout, two transgenic parental lines were time-mated. $Atrx^{flox/flox}$ females were crossed with *Forkhead box G1 (Foxg1)* $cre^{+/-}$ males, both on a C57BL6 background. Females were housed in pairs and were transferred to male's individual cages overnight for timed matings before returning to their home cages the next morning. The day of separation was considered to be embryonic day 0.5 (E0.5). All mice were housed in cages with HEPA-filtered air and allowed water and 18% Protein Rodent Diet pellets (Harlan Tekland Global Diets, Madison WI) *ad libum*.

2.3.2 Collection of embryos from timed matings

Pregnant dams at gestational days E12.5-E18.5 were anaesthetized by carbon dioxide and sacrificed by cervical dislocation. The uterus was then dissected out of the abdominal cavity and embryos were removed. Embryos were then separated from their embryonic sacs and placentas and placed in 1X Hanks' Balanced Salt Solution (HBSS).

2.3.3 Genotyping of embryos

A small piece of tissue from each individual embryo was obtained during dissection and set aside in a labeled PCR tube. Seventy five µl of alkaline lysis buffer (25 mM NaOH, 0.2 mM disodium EDTA, pH 12) was added and DNA was extracted by 30 minutes of incubation at 95°C. The reaction was then neutralized with 75 µl of neutralization buffer (40 mM Tris-HCl, pH 7.0) (Truett *et al.,* 2000). To determine the *Cre* status of each embryo, 1 µl of each sample was used for PCR amplification of *Cre recombinase* using the following primers:

Cre-Forward: 5'-ATG CTT CTG TCC GTT TGC CG -3'

Cre-Reverse: 5'-GGG CGT AGA CAT CTG GGT AG -3'

To determine the sex of each embryo, 1 µl of each sample was used for PCR amplication of *Sry* (*sex-determining region Y)* and the housekeeping gene *FABP1 (fatty acid binding protein 1).* The following primers were used:

SRY-Forward: 5'-TTG TCT AGA GAG CAT GGA GGG CCA TGT CAA -3'

SRY-Reverse: 5'CCA CTC CTC TGT GAC ACT TTA GCC CTC CGA -3'

FABP1-Forward: 5'TGG ACA GGA CTG GAC CTC TGC TTT CCT AGA -3'

FABP1-Reverse: 5'CTAG AGC TTT GCC ACA TCA CAG GTC ATT CAG -3'

The PCR mix for each reaction contained 1 µl of DNA, 40.2 µl of HPLC water, 5 µl of 10X PCR buffer, 1.5 µl of 50 mM $MgCl_2$, 1 µl of 10 mM primer pool, 1 µl of 10 mM dNTPs, and 0.3 µl of Taq polymerase (Invitrogen, Burlington ON). The reaction

conditions were as follows: 95°C for 20 sec, 57°C for 20 sec, and 72°C for 40 sec for a total of 35 cycles. Five µl of the PCR reactions were electrophoresed on a 1.5% agarose gel in 1X TAE with 0.01 µl/ml of ethidium bromide, and visualized under UV light. Reactions that were positive for both *Cre* and *Sry* were considered to be Atrx knockouts ($Atrx^{null}$).

2.3.4 Tissue fixation and Sectioning

For embryos at embryonic day 13.5 (E13.5), whole embryo heads were removed and fixed in 3 ml of 4% paraformaldehyde (PFA) in 0.1 M PBS (0.14 M NaCl, 2.5 mM KCl, 0.2 M Na_2HPO_4 and 0.2 KH_2HPO_4 at pH7.4). At E17.5 and older, the skin and skull were gently peeled back to expose the whole brain, which was then removed and fixed in the same manner as outlined above. The following day, tissue was washed three times in PBS and then sunk in 3 ml of 30% sucrose in PBS overnight for cryoprotection. Tissue was then equilibrated in a 1:1 mixture of 30% sucrose and OCT (Tissue-Tek©, Japan) for at least 1 hour before being embedded in this mixture and flash frozen on liquid nitrogen. Tissue blocks were stored at -80°C until ready for sectioning (Section 2.5.1).

2.3.5 Obtaining Tissue for Protein

Embryos were obtained as stated in Section 2.3.2. To isolate the $Atrx^{null}$ cortices, the skin and skull were peeled back and the cortices were pinched out using dissecting forceps (Dumont, Electronic Switzerland). This was performed under the magnification of a Leica MZ95 dissecting microscope. The cortices from each embryo were placed into a distinct microcentrifuge tube, flash-frozen in liquid nitrogen for 5 seconds, and stored at

-80°C until needed.

2.4 Protein time course

2.4.1 Protein Extraction

Cortices were lysed in 100-150 µl of RIPA buffer (1X PBS, 1% NP-40, 0.1% SDS, 0.5% sodium deoxycholate, protease inhibitor CompleteMini EDTA-free in ddH2O). E12.5 and E13.5 cortices were homogenized by trituration, while all older time points were homogenized for 30 seconds with the Tissue Tearor™ (Biospec Products, Inc.) All samples were then incubated on ice for at least 30 minutes. Samples were then centrifuged at 10 000 g for 10 minutes at 4°C. The supernatant was aliquoted and stored at -80°C. Before experimental use, protein concentration was determined using Bradford protein assay reagent (Bio-Rad, Mississauga, ON) and an Eppendorf BioPhotometer (Bradford, 1976).

2.4.2 SDS-PAGE and Transfer

To separate proteins by molecular weight, extracted protein samples were separated by sodium-dodecylsulfide polyacrylamide gel electrophoresis (SDS-PAGE). Samples were prepared for loading by aliquoting an equal amount of protein for each sample. The remaining volume was brought to a maximum of 40 µl with the addition of 4X NuPage® SDS Loading buffer (Invitrogen, Burlington, ON) and HPLC water. Samples were then heated at 100°C for 6 minutes and spun down before loading into a pre-cast gel (Invitrogen).

When searching for proteins $\geq$ 30 kDa, a 3-8% pre-cast gel was run with 1X NuPAGE® Tris-Acetate SDS Running Buffer (Invitrogen, Burlington, ON) at 150 V for 1.5 hours or until the dye front reached the gel foot. Proteins were transferred to a PVDF Immobilon–P Transfer Membrane (Millipore, Billerica, MA) overnight at 10 V using 1X transfer buffer (50mM Tris base, 40mM Glycine, 10% SDS, 20% MeOH). When searching for proteins < 30 kDa, a 4-12% pre-cast gel was run with MOPS buffer at 200 V for 1 hour or until the dye front reached the gel foot. Proteins were transferred for 50 minutes at 50 V on a stir plate to ensure even distribution of cold from the ice pack. 1X transfer buffer (25 mM Tris, 192 mM glycine, and 0.025% SDS) was used. After transfer, the gel was incubated with Coomassie blue (BioRad) for 20 minutes to ensure complete transfer of proteins. Protocols were obtained from the 3rd edition of "Short Protocols in Molecular Biology", edited by Ausubel et al., 1995.

2.4.3 Immunoblots

Each membrane was incubated in blocking buffer (5% milk in TBS-T) for 1 hour. Primary antibody was diluted to the appropriate concentration (see Table 3) in blocking buffer and the membrane was incubated for either 2 hours at room temperature or overnight at 4°C. The membrane was then washed five times for 5 minutes each in 1X TBS-T and incubated in secondary antibody diluted in blocking buffer (see Table 3) for 45 minutes at room temperature. The membrane then received five more 5 minute washes in 1X TBS-T followed by two 5 minute washes in 1X PBS. Proteins were detected by enzymatic chemiluminescence using the Sigma-Alderich ECL kit (GE Healthcare, Buckinghamshire UK). In instances where membranes were probed sequentially with multiple antibodies, the membrane was stripped for 30 minutes in a

Table 3: A summary of antibodies used and their specific conditions.

Protein of Interest	Host animal	Company	Technique	Dilution
Primary Antibodies				
AIF	Goat	Santa Cruz	WB	1: 500
Atrx (F39)	Mouse	homemade	WB	1:3-1:6
Atrx (H300)	Rabbit	Santa Cruz	IHC, ICC	1: 100
β-actin	Mouse	Sigma-Alderich	WB	1: 10 000
γ-H2AX	Rabbit	Cell Signalling	WB, IHC	1: 2 000, 1: 200
Par	Rabbit	BD Pharmingen	WB	1: 2 000
Par	Mouse	Trevigen	IHC, ICC	1: 200
Parp-1	Mouse	BD Pharmingen	WB	1: 2 000
p53	Mouse	Cell Signalling	WB	1: 2 000
Reelin	Mouse	Cell Signalling	IHC	1:1 000
Secondary Antibodies				
-	Sheep α mouse	Sigma-Alderich	WB	1: 2 500
-	Goat α rabbit	Sigma-Alderich	WB	1: 4 000
-	Rabbit α goat	Sigma-Alderich	WB	1: 5 000
-	Goat α rabbit-594	Invitrogen	IHC, ICC	1: 10 000
-	Donkey α mouse-488	Invitrogen	IHC, ICC	1: 10 000

rotating incubator at 50°C in stripping buffer (100 mM β-mercaptoethanol, 2% SDS, 62.5mM Tris-HCl pH 6.7). Before probing with another antibody, the membrane was washed briefly in TBS-T and blocked again for 1 hour.

2.4.4 Densitometry Analysis of Western Blot

In order to quantify Parp-1 activity from Western blots, densitometry analysis was performed using ImageJ software (National Institutes of Health, USA). Pixelation of Western blot signal levels for Parp-1 and Par were measured in aribitrary units. Background levels were subtracted and the Par values were normalized to output values of Parp-1. These values were graphed with the use of Microsoft Excel.

2.5 Immunohistochemical Analysis of Tissue Sections

2.5.1 Sectioning of Tissue

Tissue blocks were allowed to equilibrate at -21°C in a Leica 1850 cryostat for 30 minutes. Excess OCT was cut from around tissue as desired and the block was mounted to a cutting platform using OCT. Tissue was then serially sectioned in 10 μm increments and mounted on Superfrost Plus coated slides (Fisher Scientific, USA). $Atrx^{null}$ and wildtype samples were both mounted on each slide to minimize possible experimental error between genotypes during staining. Slides were allowed to dry at room temperature for 2 hours before being stored at -20°C in a slide box with a teaspoon of desiccant.

2.5.2 Par Immunohistochemistry

The slide box was removed from -20°C and allowed to equilibrate at room

temperature for 1 hour before opening and exposing slides. Slides were first fixed with 70% ethanol for 5 minutes and then rehydrated in 1X PBS for 5 minutes. When probing for Par, slides were incubated in 2N HCl for 20 minutes at 37°C. This was followed by a 10 minute wash in 0.1 M Tris (pH 8.8) + 0.1% Tween-20 and three 5 minute washes in 1X PBS washes. All tissue sections were then outlined with a hydrophobic marker (Dako). An excess of blocking buffer (20% goat serum, 0.3% Triton-X in PBS) was pipetted onto sections and incubated at room temperature in a humid chamber for 1 hour. Block was drained from slides and the primary antibody was diluted in blocking buffer and added overnight at 4°C in a humid chamber. Antibodies and concentrations are listed in Table 3. The following day, slides received three 10 minute washes in 1X PBS and were then incubated in secondary antibody (diluted into TBLS) for 1 hour at room temperature in a darkened humid chamber. Slides were washed for 10 minutes in 1X PBS and then incubated in the dark with DAPI for 4 minutes. Slides were washed three times for 10 minutes each in 1X PBS and then mounted with DAKO fluorescence protector. Sections were examined on a Zeiss Axioplan microscope and digital images were captured using an AxioVision 6.05 (Zeiss) camera.

2.6 Primary Neurosphere Cultures

2.6.1 Generation of Neurospheres

A pregnant dam at gestational stage E12.5 was sacrificed and her embryos were extracted as per Section 2.3.2. Embryo cortices were removed under the dissection microscope and placed in pre-cooled microcentrifuge tubes on ice. Cortices were triturated in 500 µl of proliferation media (Neurocult NSC proliferation supplements, 20

ng/ml recombinant human EGF [Invitrogen], 0.5% antimycotic/antibiotic in Neurocult NSC Basal Medium [StemCell Technologies]). Once the suspension was uniform, this 500 µl was added to 19.5 ml of proliferation media in a T75 flask. Cultures were monitored for the next several days for the formation of spheres.

2.6.2 Neurosphere Differentiation

Coverslips were pretreated with 1 ml of 1X PDL and 15 µg/µl of laminin in sterile PBS for 3 hours. Proliferating neurospheres were spun down at 800 rpm in a table top Heraeus Instruments Megafuge 1.0 for 5 minutes and the pellet was resuspended in PBS for plating. A portion of neurospheres were allotted into wells or plates containing differentiation media (Neurocult NSC Differentiation Supplements [StemCell Technologies], 1% antibiotic/antimycotic Neurocult NSC Basal Medium [StemCell Technologies]) and allowed to incubate at 37°C for the desired amount of time; either 1, 3, 5, or 7 days of differentiation.

2.6.3 Harvesting Neurospheres for Protein

Neurospheres from Days 0, 1, 3, 5, and 7 of differentiation were gently pipetted from their 10 cm plates into falcon tubes, leaving a small amount of media in the dish. Remaining cells were scraped and pooled into remaining media, which was then transferred into the falcon tube. Cells were centrifuged at 800 rpm for 5 minutes and the media was aspirated off the pellet. Cells were washed with 1X PBS, recentrifuged, the 1X PBS was removed and the pellet was then stored at -80°C or used for experimental purposes. The protocol outlined in Section 2.4.1 was followed, with each cell pellet being

lysed in 150 µl of RIPA buffer.

2.7 Nuclear protein fractionation

Cortices from E12.5 and E17.5 embryos were obtained as outlined in Section 2.3.5. Cortices were then lysed in 200 µl of lysis buffer A (10 mM HEPES pH 7.5, 10 mM NaCl, 1.5 mM $MgCl_2$, 10% glycerol, 1 mM EDTA, 5 mM DTT, 1% NP-40) with careful trituration. Samples were then briefly vortexed and centrifuged at 1 000 g for 5 minutes at room temperature. The supernatant containing the cytoplasmic protein fraction was transferred to a new microcentrifuge tube and stored on ice. The nuclear pellet was gently washed with lysis buffer A (excluding NP-40) and was vortexed and centrifuged again. The supernatant was discarded and the nuclear pellet was resuspended in 50 µl of nuclear lysis buffer (25 mM Tris-HCL pH 8.0, 500 mM NaCl, 1 mM EDTA, 10 mM β-mercaptoethanol, 0.5% Triton-X). Samples were briefly vortexed and centrifuged at 30 000 g for 30 minutes at 4°C. The supernatant containing the nuclear protein was transferred to a new microcentrifuge tube and the pellet was discarded. Protein concentrations were measured by Bradford assay.

2.7 Assessment of DNA damage

2.7.1 γ-H2AX Western blots

To assess whether $Atrx^{null}$ embryos had increased DNA damage in the cortex, γH2AX levels were assessed by Western Blot in a cortical protein time course with $Atrx^{null}$ and wildtype protein from ages E12.5, E15.5, and E17.5. As a positive control, UV damage was induced on HEK293 cells at 80-100% confluency. Media was aspirated

and replaced with 2-3 ml of PBS to keep cells hydrated, and the plate was left uncovered under the Biosafety cabinet's UV light for 1 minute (~114 J/m^2). Media was then replenished and the cells were allowed to recover for 2 hours at 37°C. At this time, media was aspirated and cells were trypsinized for 5 minutes before being pelleted at 1 200 rpm in a table top Heraeus Instruments Megafuge 1.0 for 5 minutes. As a negative control, untreated HEK293 cells were used. All protein extractions were performed as outlined in Section 2.4.1.

2.7.2 γ-H2AX Immunohistochemistry

When staining for γH2AX, the immunohistochemistry (IHC) protocol outlined in Section 2.5.2 was followed, however in lieu of an HCl treatment, E13.5 sections received a 5 minute microwave treatment in a 1X sodium citrate antigen retrieval solution (0.01 M citric acid, 0.025 M NaOH pH 6.0) on Power setting 5. Slides were washed twice for 5 minutes in 1X PBS and the rest of the protocol in Section 2.5.2 was followed.

2.9 Cortical Layer Molecular Marker Study

In order to determine if neurons from a particular cortical layer were dying in the Atrx^{null} cortex, a molecular marker study of the cortical layers was performed. Wildtype and Atrx^{null} brains from E18.5 embryos were sectioned as described in Section 2.5.1. The layers were examined either by IHC or *in situ* hybridization, and the markers used are listed in Table 3.

2.9.1 Immunohistochemistry

When staining for the Layer I marker Reelin, IHC was performed as outlined in

Section 2.5.2. However, no HCl treatment or antigen retrieval step was required. The dilution used is listed in Table 3.

2.9.2 *In situ* hybridization

To study cortical layers II-VI, *in situ* hybridization was performed for the following markers: SG10 (II, III, IV, V), Er81 (V), Otx1 (V), and Tbr1 (VI). Protocol is described by Jensen and Wallace (2007) and probe conditions are listed in Table 4. Probes stored at -80°C were thawed quickly and diluted to 1:1 000 in hybridization buffer (50% formamide, 10% dextran sulfate, 1 mg/mL yeast tRNA, 1x Denhardt's and 1x SSC). Diluted probes were then denatured at 70°C for 10 minutes, vortexed vigorously, and 150 µl was pipetted onto the slide before covering with a coverslip. Slides were placed in a humid chamber and incubated overnight at 65°C in a dry oven. Post-hybridization, slides were transferred to a glass slide rack and sections were incubated for 15 minutes on a rocking platform in Wash buffer (50% formamide 1X SSC, 0.1% Tween-20) that had been pre-warmed to 65°C. Wash buffer was refreshed twice, each after a 30 minute incubation. Slides were then incubated twice for 30 minutes in 1X MABT (100 mM maleic acid, 150 mM NaCl, pH 7.5, 0.1% Tween-20) with rocking. At this point, slides were outlined with a hydrophobic marker and transferred to a humid chamber containing Whatmann paper saturated with PBS. Blocking solution (20% heat-inactivated sheep serum, 2% blocking reagent in 1X MABT) was added to the sections which were then allowed to incubate for 1 hour at room temperature. Once the block was aspirated, 150 µl of anti-DIG antibody, diluted 1:1 500 in block, was pipetted onto the sections and incubation proceeded overnight at 4°C. The following morning, slides were transferred from the humid chamber to a glass slide rack. Slides were then washed five

Table 4: A summary of the cortical layer markers used and their specific conditions.

Immunohistochemistry		
Antibody	**Dilution**	**Layer(s) marked**
Reelin	1: 1 000	I
In situ hybridization		
Probe	**Dilution**	**Layer(s) marked**
SG10	1: 1 000	II, III, IV, V
Er81	1: 1 000	V
Otx1	1: 1 000	V
Tbr1	1: 1 000	VI

times with 1X MABT for 20 minutes each with rocking. Coverslips fell away from slides after the first wash. Sections were then equilibrated in Post-antibody Wash Buffer (100 mM NaCl, 50 mM MgCl2, 100 mM Tris pH 9.5 and 0.1%-Tween 20) twice for 10 minutes each at room temperature with rocking. To begin the colour reaction, slides were placed in a glass coplin jar filled with 30 ml of Staining Buffer (100 mM NaCl, 50 mM MgCl2, 100 mM Tris pH 9.5, 0.1%-Tween, 4.5 µl/mL 4-Nitro blue tetrazolium chloride [Roche], 3.5 µl /mL 5-bromo-4chloro-3indolyl-phosphate [Roche]). This reaction was allowed to incubate in the dark at room temperature. After 2 hours, sections were checked periodically under the microscope for the development of colour. Depending on the probe, this reaction took between 2 hours and overnight. To stop the staining reaction, slides were removed from Staining Buffer and washed three times for 5 minutes each in 1X PBS before being mounted with a 1:1 mixture of glycerol: 1X PBS and stored at 4°C. Sections were examined on a Zeiss Axioplan microscope and digital images were taken using an AxioVision 6.05 (Zeiss) camera and processed using Adobe® Photoshop.

2.10 Parp-1 Inhibitor Study

In order to determine if suppression of Parp-1 activation would have an effect on the neuronal death observed in *Atrx*^{null} mice, timed mated mice were injected with a Parp-1 inhibitor. Mice were weighed on the day of injection, and the inhibitor PJ34 (Calbiochem) was diluted in sterile 1X PBS in order to prevent the elongation of any Parp-1-induced PARylation. A variety of dosages was attempted via intraperiteneal injection:

- 1 mg/kg at E10.5
- 1 mg/kg at E9.5
- 5 mg/kg at E9.5
- 1 mg/kg at E10.5 + 1 mg/kg at E12.5

Control mice received an injection of 1X PBS at the same time points as treated mice. At E13.5, the pregnant dams were sacrificed and their cortices were dissected (Section 2.3.5) and the protein was extracted (Section 2.4.1). Genotyping and Western blot were performed to confirm $Atrx^{null}$ status.

3.0 Results

3.1 Characterization of Parp-1 during neurogenesis

A topic that is currently absent from the literature regarding this project is the general characterization of Parp-1 throughout cortical development. Since both ATRX and PARP-1 are proteins that have roles in the life and death of neurons, their expression was monitored both *in vitro* and *in vivo* during neurogenesis.

3.1.1 Increased Parp-1 expression *in vitro* during growth and early differentiation

Initial *in vitro* work involved screening for Parp-1 expression in differentiating populations of N1E115 cells—a mouse neuroblastoma cell line. Protein was extracted from N1E115 cells that had differentiated from Days 0-7. It was observed that Parp-1 expression was highest during growth (Figure 9). Parp-1 expression was also strongly visible by Western blot at days 1, 2, and 3 of differentiation. Expression levels decreased significantly from day 4, and after day 7 there was no Parp-1 visible.

3.1.2 Increased Parp-1 activity *in vivo* during early corticogenesis

In order to further our knowledge of the expression patterns of Parp-1 during development, Parp-1 and Par expression levels were monitored in the cortex of wildtype mice. Embryos of ages E12.5-P0 were dissected and genotyped, and brains were either fixed and sectioned or the cortices were flash-frozen and used for protein. Western blot showed that Parp-1 expression was mainly steady throughout development, although

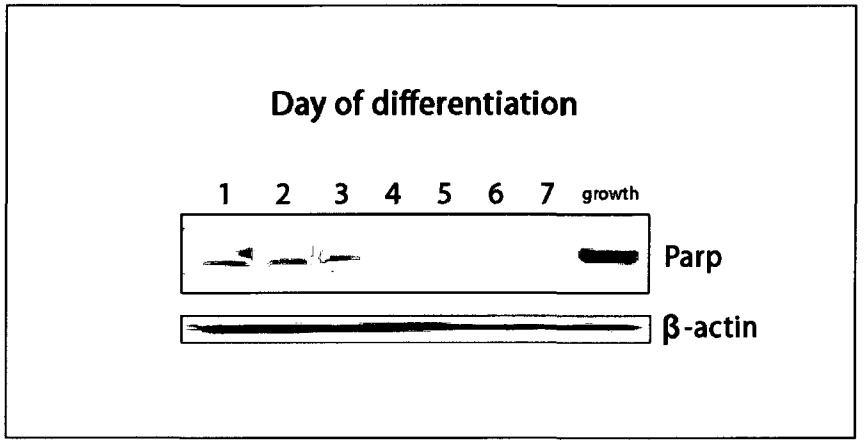

Figure 9: Parp-1 expression levels in differentiating mouse neuroblastoma cells
Western blot analysis was performed to monitor Parp-1 expression of protein isolated from N1E115 cells at days 0-7 of differentiation. β-actin was used as a loading control. Increased Parp-1 expression levels were identified in growth and in early days of differentiation. (N=3).

levels seemed subtly lower towards the end of corticogenesis (Figure 10, third panel, lanes labeled **WT**). Attempts to examine Parp-1 levels by IHC were unsuccessful.

In order to gauge Parp-1 activation, levels of Par were assessed. By Western blot analysis, a striking increase in Parp-1 activation is seen at early stages of development (Figure 10, second panel, **WT** lanes). Specifically, the largest amount of Parp-1 activity is found at the earliest assessed points of development, and levels drop off at E17.5. Analysis by IHC further confirmed this finding, and quantification of Par^+ cells show 46.8 % $\pm$ 6.2% of cells to be positive for Parp-1 activity at E13.5, and these Par^+ cells are evenly distributed throughout the developing cortex (Figure 11, first panel).

3.2 Characterization of Parp-1 activity in the $Atrx^{null}$ cortex

3.2.1 Increased Parp-1 activity in $Atrx^{null}$ mice compared to wildtype littermates

In order to inspect potential trends of Parp-1 expression in the $Atrx^{null}$ cortex, timed matings were established between $Atrx^{f/f}$ females and male mice ($Atrx^{wt/y}$; Foxg1 $cre^{+/-}$) to obtain $Atrx^{null}$ embryos at ages E12.5-P0. These embryos were dissected and genotyped, and $Atrx^{null}$ embryos were either fixed and sectioned or their cortices were flash-frozen and used for protein extraction. This portion of the project was performed in conjunction with Section 3.1.2, using the various genotypes of a litter. Western blot was used to look at levels of both Parp-1 expression and Parp-1 activity (Figure 10). These time course experiments show that levels of Parp-1 are not altered from wildtype levels in the absence of Atrx, and interestingly, Parp-1 cleavage is not observed despite the enhanced apoptosis that occurs in $Atrx^{null}$ embryos. However, Parp-1 activity detected by

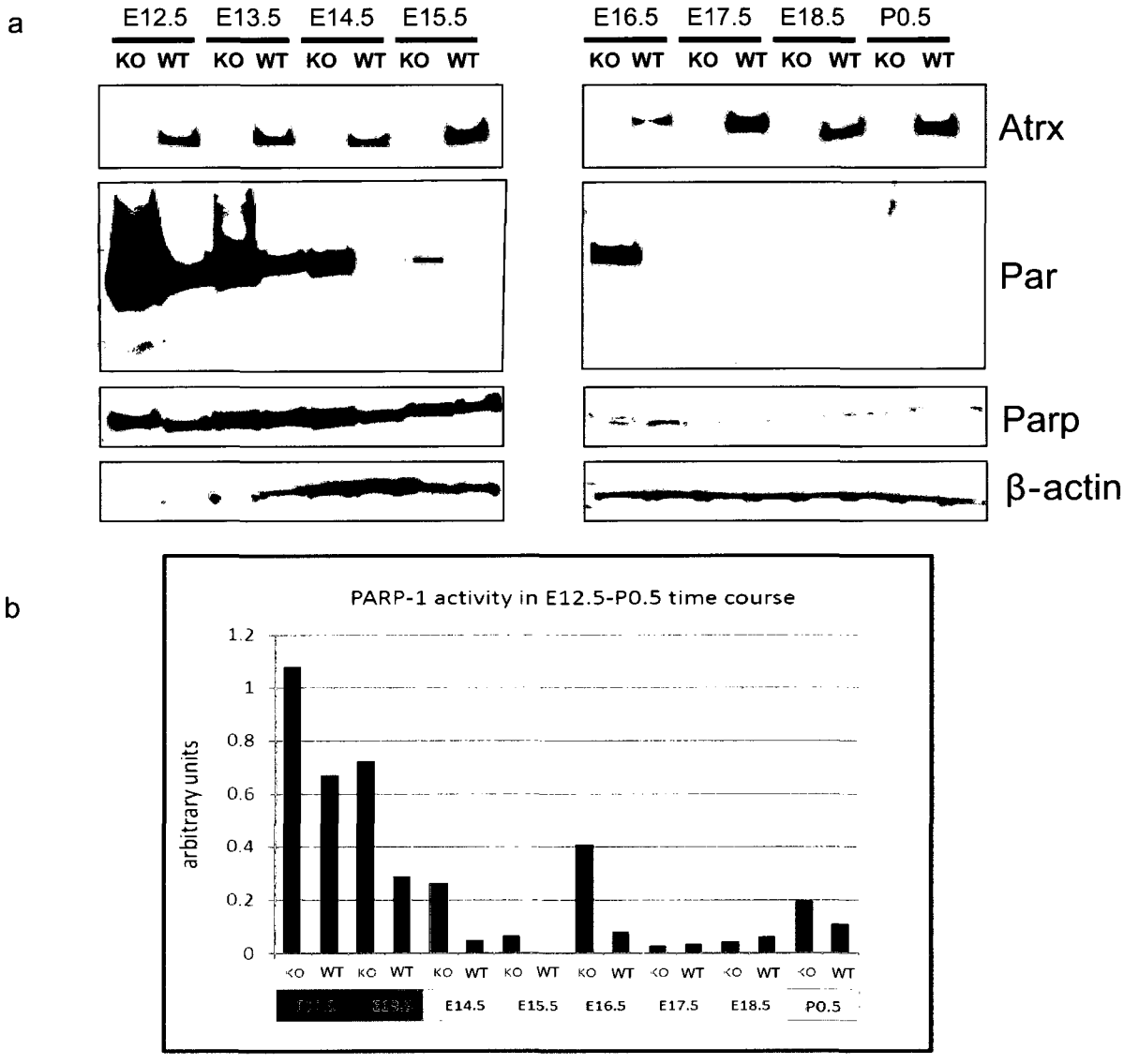

Figure 10: Differentiation time course of wildtype and Atrx^{null} cortical protein
(A) Western blot analysis was performed to monitor levels of Parp-1 expression and activation in protein isolated from both Atrx^{null} and wildtype cortices from ages E12.5-P0.5. Atrx status was confirmed and β-actin was used as a loading control. Parp-1 expression levels decrease in both genotypes over the course of corticogenesis. Parp-1 activity, as measured by Par expression, is dramatically increased in the Atrx^{null} cortex compared to wildtypes at early embryonic time points. Par levels also persist through embryonic development in Atrx^{null} samples when levels are barely detectable in wildtype littermates. (N=3). *WT=wildtype; KO=Atrx*^{null}. **(B)** Densitometry analysis was performed using Image J software in order to quantify Parp-1 activity. Pixelation of Western blot signal levels for Parp-1 and Par were measured in aribitrary units. Background levels were subtracted and the Par values were normalized to output values of Parp-1.

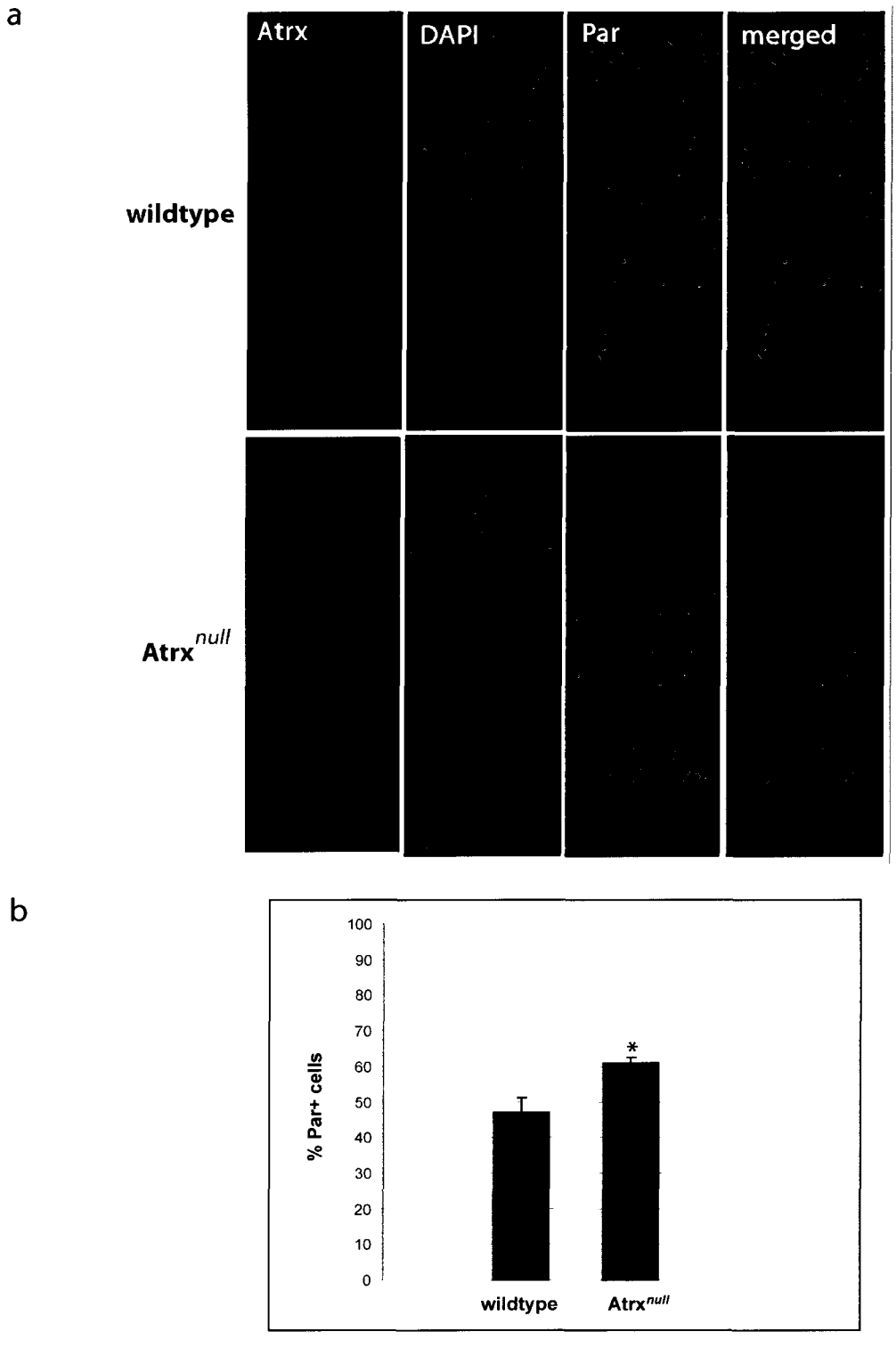

Figure 11: Immunohistochemical analysis of Parp-1 activity in the E13.5 cortex
(A) Cortical tissue sections from E13.5 Atrx^{null} and wildtype embryos were stained with antibodies against Par (green) and counter stained with DAPI (blue). This figure demonstrates an increased number of Par positive cells in the Atrx^{null} cortex compared to the wildtype cortex (magnification: 20X). **(B)** Analysis of the quantification of Par positive cells showed there was a statistically significant increase in Parp-1 activity in the E13.5 Atrx^{null} cortex versus wildtype ($p \leq 0.05$). Error bars represent SEM. ($N_{Atrx}{}^{null}=3$, $N_{wt}=2$, Student T-Test analysis).

staining for Par is dramatically increased in the Atrx^{null} cortex compared to wildtype mice; most obviously at early embryonic time points. Increased Par expression levels also persist through embryonic development in Atrx^{null} forebrains even when levels are barely detectable in wildtype littermates. This is further confirmed through densitometry analysis (Figure 10b).

3.2.2 Parp-1 activity is increased in the E13.5 Atrx^{null} mouse cortex

Immunohistochemistry to examine Parp-1 activity was performed on E13.5 cortical sections, and Par$^+$ cells were quantified (Figure 11). Upon quantification we observed that 46.8 % ± 6.2 % of the wildtype cortex contained Par$^+$ cells, whereas 61.0 % ± 2.7 % of the cells in the Atrx^{null} cortex were Par$^+$. This was a statistically significant change as determined by a two-tailed student's t-Test (n_{wt}=2, n_{ko}=3, ± SD, $p<0.05$). By E17.5, Par$^+$ cells are almost completely absent when monitored by IHC, with only a very diffuse staining present in a small portion of Atrx^{null} cells (Figure 12). This is consistent with what is observed by Western blot. Furthermore, there were many more Par$^+$ (green) cells lining the ventricle, suggesting that cells undergoing mitosis may be activating Parp-1.

3.3 Characterization of Parp-1 expression in neurosphere populations

In order to better study the ATR-X syndrome, an *in vitro* model would be of great benefit. In an attempt to solidify primary neurospheres as such a model, several wildtype and Atrx^{null} neurosphere lines were established and Parp-1 activity was characterized. Western blot analysis shows high levels of Parp-1 activity during growth and early differentiation, which is consistent with what is seen in cortical protein extracts.

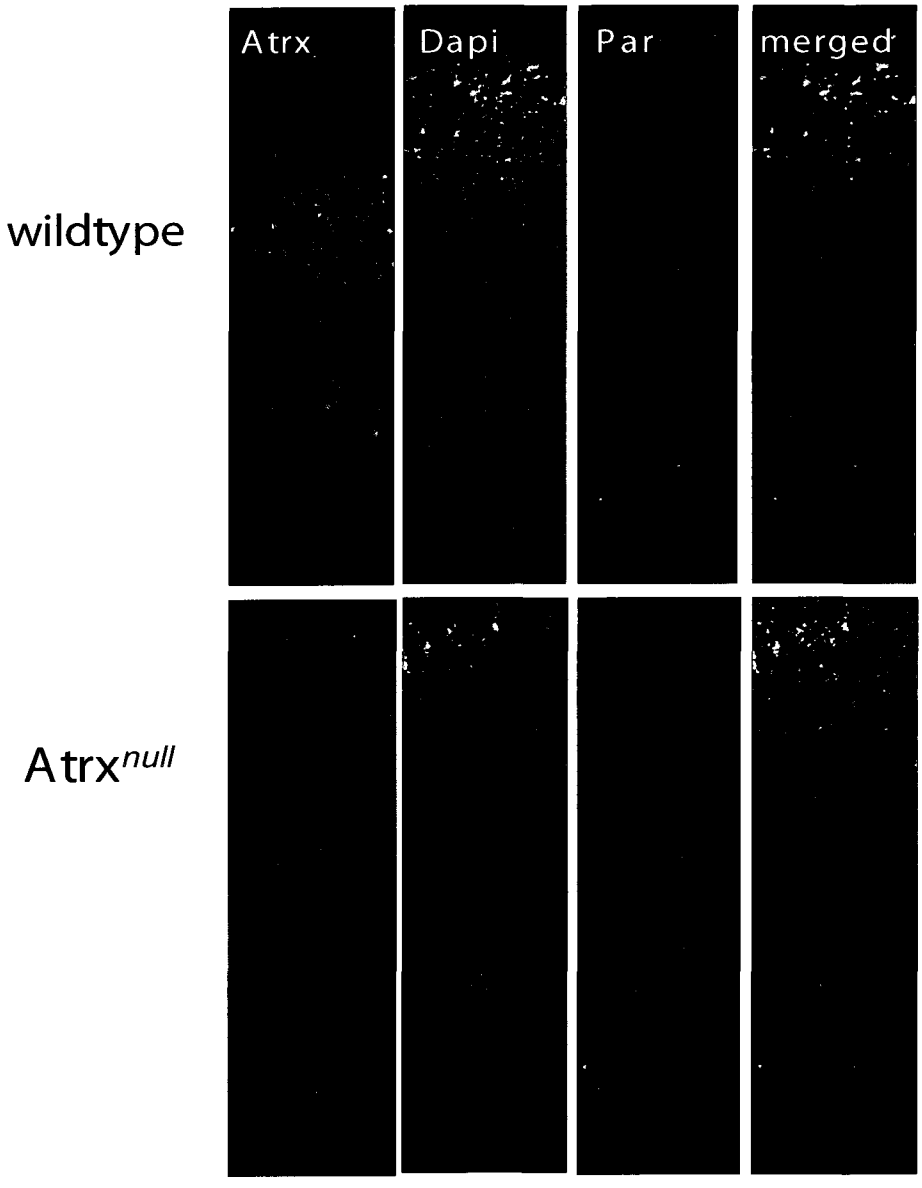

Figure 12: Immunohistochemical analysis of Parp-1 activity in the E17.5 cortex
Cortical tissue sections from E17.5 Atrx^{null} and wildtype embryos were stained with antibodies against Par (green) and counter stained with DAPI (blue). This demonstrates very little Par staining in both the Atrx^{null} cortex and wildtype cortex (magnification: 20X). Tissue sections were on the same slides as tissue from Figure 11, which thus acted as a positive control (N=3).

Quantification of immunocytochemistry (ICC) experiments reveals the largest amount of Par^+ cells at Day 1 of differentiation, and by Day 7 there are no Par^+ cells. However, in contrast to the cortical experiments, we do not observe the persistence of Parp-1 activity in $Atrx^{null}$ cultures throughout differentiation, and so neurospheres were not pursued further as a model (Figure 13). The remaining experiments were thus performed with cortical samples.

3.4 Investigation into the mechanism of Parp-1 involvement in $Atrx^{null}$ phenotype

In an attempt to explore the mechanism of Parp-1 activation when Atrx is ablated from the murine cortex, both fractionation experiments and the assessment of DNA damage in the cortex were pursued. The $Atrx^{null}$ cortex has been shown to have a 12-fold increase in apoptosis at E11.5 and a 4-fold increase at E13.5 (Bérubé et al., 2005). However, previous caspase 3 fluorometric assays performed in our lab show that while there is a statistically significant increase in caspase 3 activity in the $Atrx^{null}$ cortex as compared to wildtypes, there is still not a huge amount of overall activation (E. Goodall, unpublished). This suggests that caspase-dependent pathways may not be the only apoptotic pathways contributing to the observed neuronal death, and warrants further study into caspase-independent apoptosis. Similarly, the lack of Parp-1 cleavage suggested that other apoptotic mechanisms may be active.

3.4.1 Investigation of caspase-independent apoptosis in the $Atrx^{null}$ cortex

To determine if Parp-1 is activated as part of an apoptotic cascade, Apoptosis

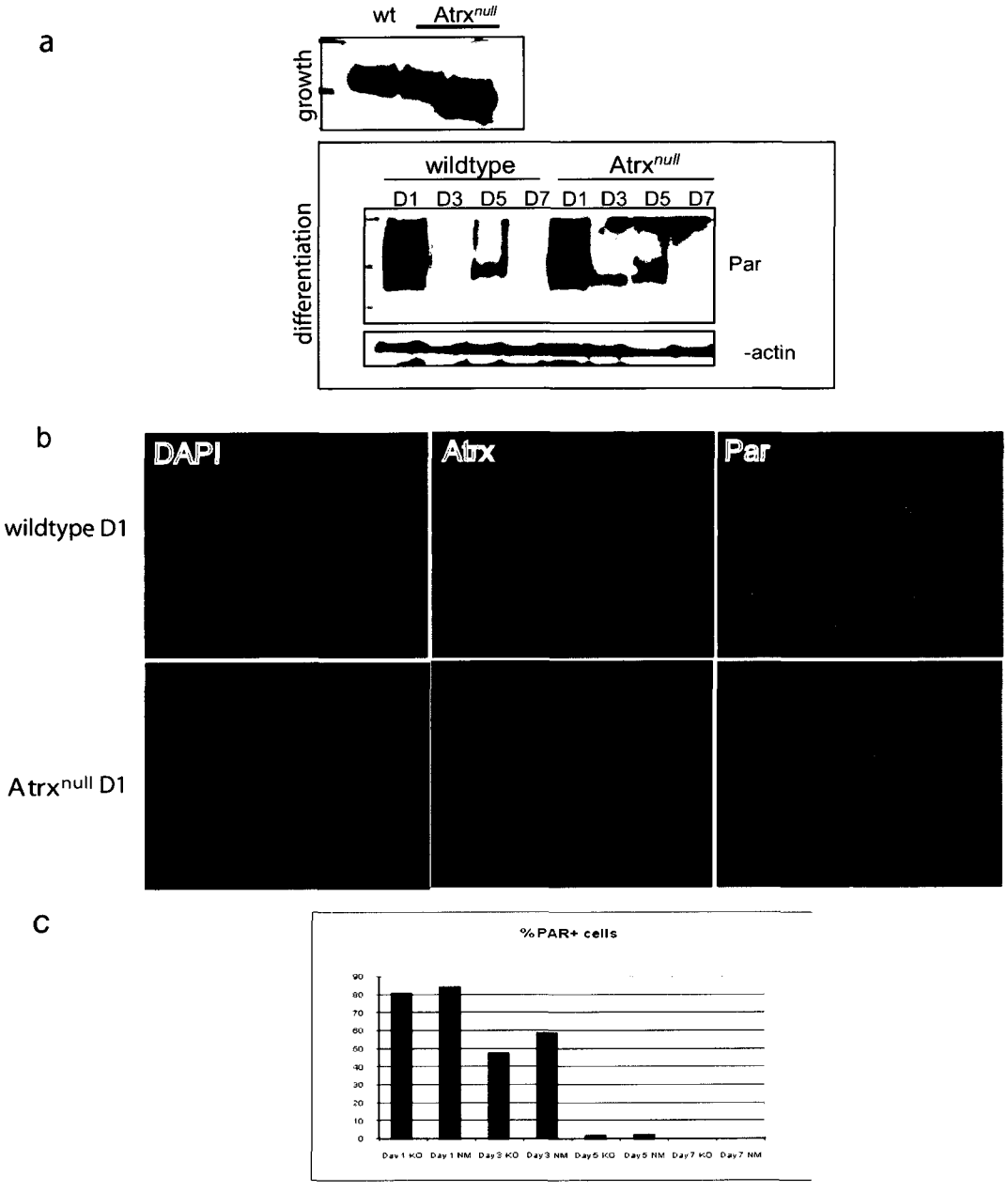

Figure 13: Parp-1 activation in differentiating neurosphere populations
(A) Par expression levels were monitored by Western blot in protein from differentiating populations of neurospheres derived from Atrx^{null} and wildtype cortices. Higher levels of Par expression are found during growth and early differentiation, but there is no difference in Parp-1 activity between genotypes. (N=3). **(B)** Cell staining of neurospheres at Day 1 of differentiation. Antibodies against Atrx (red) verified Atrx^{null} status of the cultures. Antibodies were used against Par (green) and cells were counter stained with DAPI (blue). This demonstrates that there is no obvious difference in Parp-1 activity in neurospheres when Atrx is missing (magnification: 40X). **(C)** Analysis of the quantification of Par positive cells showed there was no statistically significant difference in Par positive cells in Atrx^{null} neurospheres versus wildtypes.

Inducing Factor (AIF) needed to be examined. In response to the activation and automodification of Parp-1, AIF can translocate from the mitochondria to the nucleus to induce a caspase-independent form of apoptosis (Yu et al., 2002). To investigate this pathway, cellular fractionation and subsequent Western blot experiments were completed with wildtype and Atrx^{null} protein extracts from E13.5 and E.17.5 mice. Antibodies for AIF show no translocation to the nucleus, indicating that it is not detectably involved in the Atrx^{null} phenotype (Figure 14). Antibodies for p53 show that the protein remains nuclear and at low levels, as is typical, and is not stabilized in the absence of Atrx throughout our timecourse.

3.4.2 Investigation of DNA damage in the Atrx^{null} cortex

PARP-1 is best known as a cellular player in response to DNA damage, so we investigated whether Parp-1 activation in the Atrx^{null} cortex was in response to DNA damage. To determine if there is increased DNA damage in the Atrx^{null} cortex, levels of the DNA damage marker phosphorylated H2AX (γH2AX) were monitored by Western blot and IHC. Western blot analyses show increased levels of γH2AX in Atrx^{null} cortices compared to wildtype during early stages of corticogenesis (Figure 15a). γH2AX is absent in both genotypes at more perinatal time points. The time points exhibiting damage correspond to those where an increase in Parp-1 activity is seen. IHC for γH2AX at E13.5 confirms this increase and also shows that the majority of cells incurring DNA damage are located in the progenitor region of the cortex (Figure 15b). Upon quantification we observed that 7.2 % ± 5.5 % of the wildtype cortex contained γH2AX+ cells, whereas 22.8 % ± 3.3 % of the cells in the Atrx^{null} cortex were γH2AX+. This was a statistically significant change as determined by a two-tailed student's t-Test (n=3, ± SD

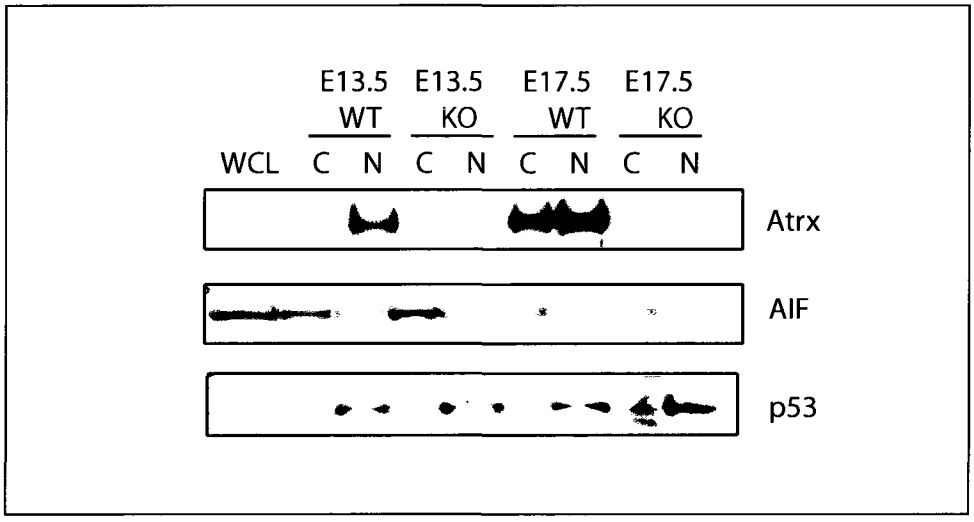

Figure 14: Fractionation of E13.5 Atrx^{null} and wildtype cortical protein
Protein fractionation and subsequent Western blot analysis was performed to monitor the cellular location of AIF in protein isolated from both Atrx^{null} and wildtype cortices at ages E13.5 and E17.5. Atrx status was confirmed. p53 levels are also steady and remain nuclear.AIF expression is consistent and does the protein does not appear to translocate from the cytoplasm to the nucleus to induce caspase-independent apoptosis. (N=3). *WT=wildtype; KO=Atrx*^{null}

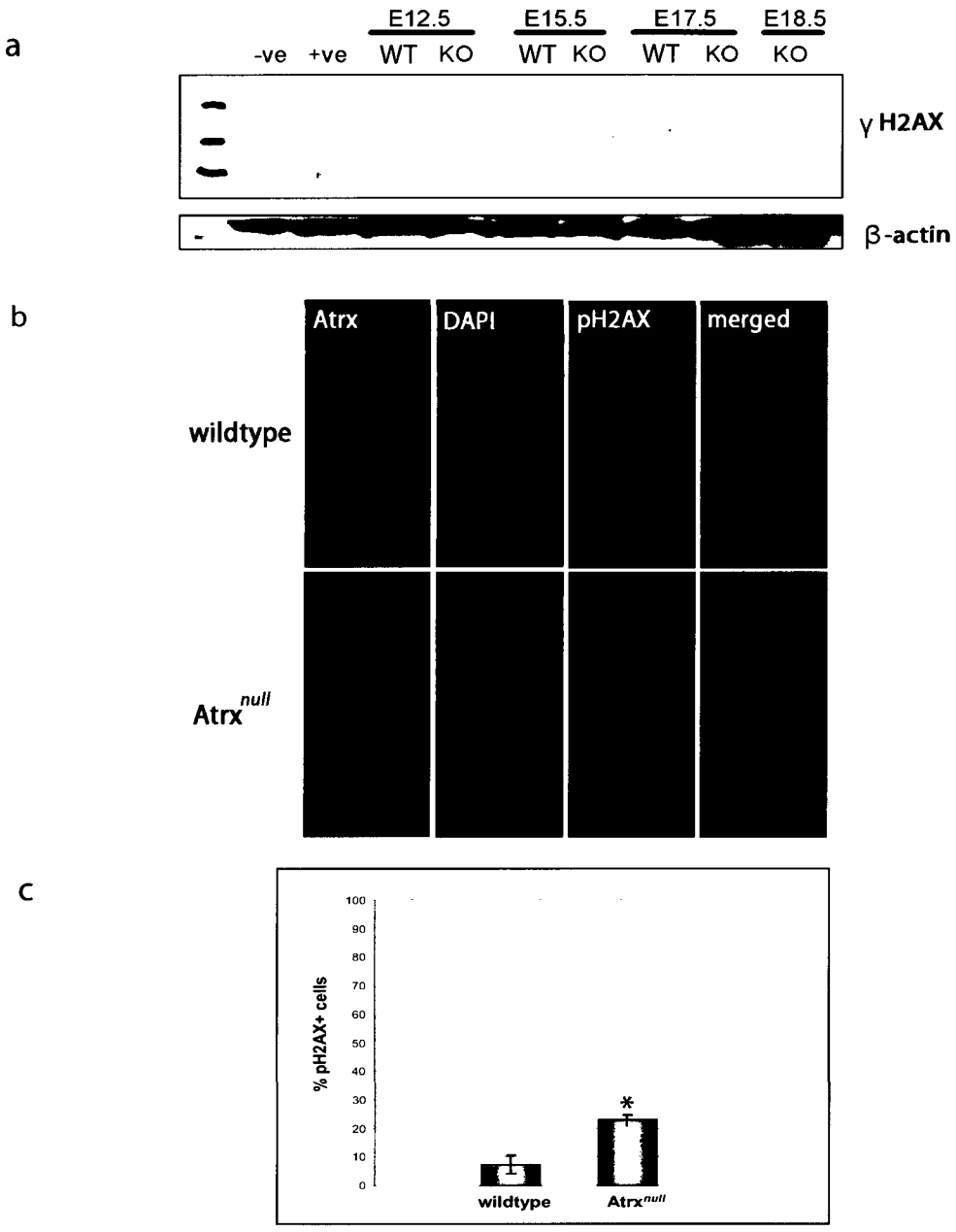

Figure 15: Analysis of DNA damage in the E13.5 cortex

(A) γH2AX expression was monitored by Western blot and exhibits higher expression in the Atrx^{null} cortex versus the wildtype cortex at E12.5 and E15.5. Expression is detected in neither the Atrx^{null} or wildtype cortex at E17.5 or E18.5. Atrx status was confirmed by Western blot (data not shown). Antibody specifications are listed in Table 3. (N=3). **(B)** Cortical tissue sections from E13.5 Atrx^{null} and wildtype embryos were stained with antibodies against γH2AX (red) and counter stained with DAPI (blue). Atrx^{null} status was verified by IHC. This demonstrates an increased number of γH2AX positive cells in the Atrx^{null} cortex compared to the wildtype cortex (magnification: 20X). **(C)** Analysis of the quantification of γH2AX positive cells showed there was a statistically significant increase in γH2AX positive cells in the E13.5 Atrx^{null} cortex versus wildtype ($p \leq 0.05$). Error bars represent SEM. (N=3, Student t-Test analysis). *WT=wildtype; KO=Atrx*^{null}*; +ve control = UV-treated HEK293 cells; -ve control = untreated HEK 293 cells.*

$p<0.05$). This result suggests that in the absence of Atrx, the murine cortex is more prone to DSBs.

3.5 Investigation of changes in cortical neuron number in the layers of the Atrx^{null} cortex

Since the Atrx^{null} cortex has been shown to have both cell death and DNA damage occurring early in corticogenesis, a molecular marker study was performed in E18.5 Atrx^{null} forebrains to determine if the cell loss was general or specific to one or more of the six cortical layers. Both IHC and *in situ* studies were performed on E18.5 brain sections, and the layer markers listed in Table 4 were examined in both rostral and caudal coronal sections of the cortex. Rostral and caudal sections were chosen as the Atrx^{null} phenotype is more severe in caudal regions of the cortex. All Atrx^{null} layers showed normal expression patterns of the markers with the exception of Er81 (Figure 16). Decreased expression of this particular transcription factor was found throughout the cortex, but was most noticeable in the caudal region. This represents a reduction in a subpopulation of layer 5 neurons. Additionally, layer 6 neurons remain present but appear to be less ordered in the caudal region of the cortex, as evidenced by the marker Tbr1. Layer 5 and layer 6 neurons are born between E11.5 and E14.5—a range corresponding to a large portion of the neuronal death that is observed in the Atrx^{null} cortex.

3.6 Parp-1 inhibitor study

To further understand the role of Parp-1 in the Atrx^{null} cortex, a Parp-1 inhibitor

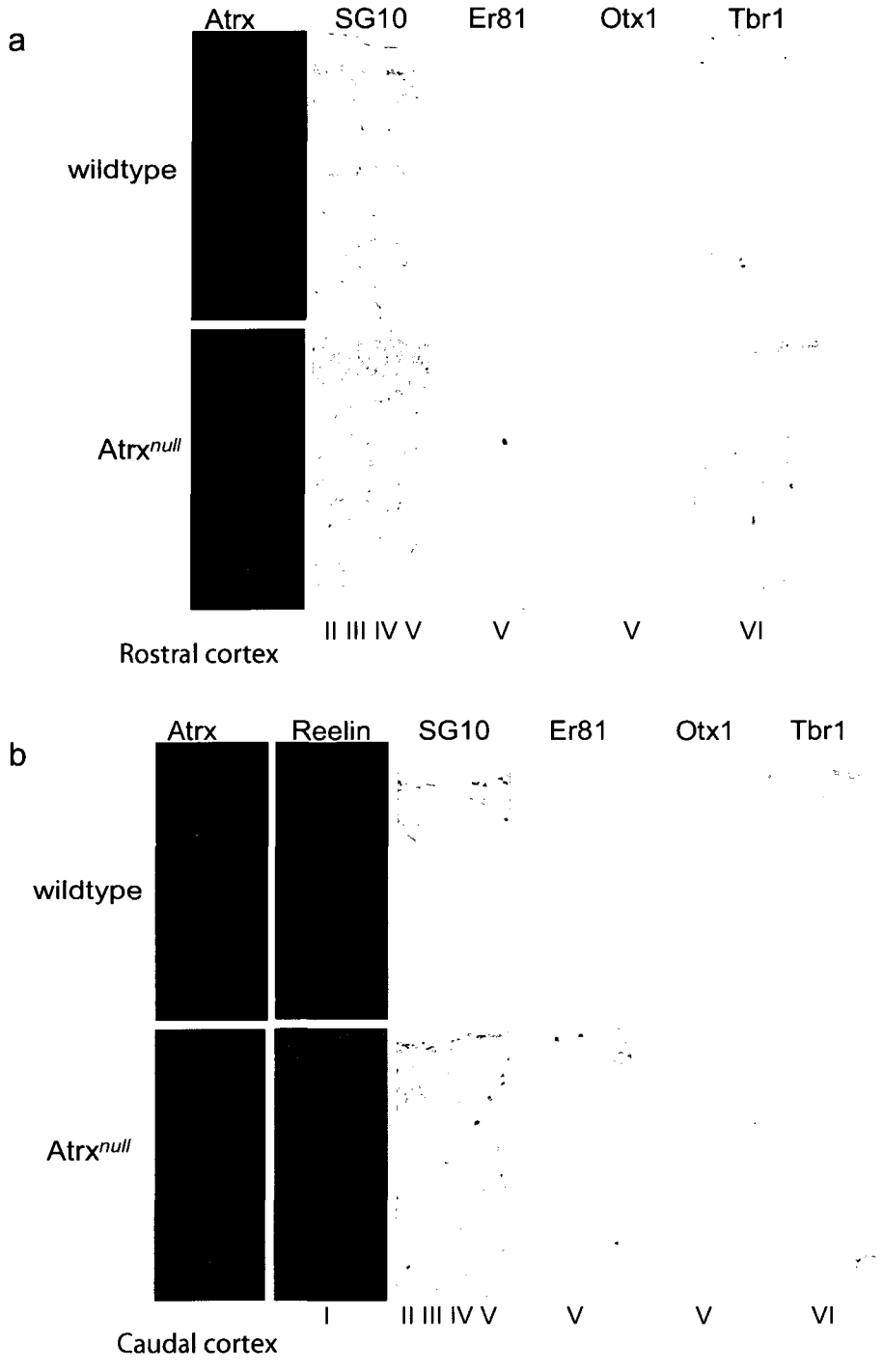

Figure 16: Molecular marker characterization of the Atrx^{null} and wildtype E18.5 cortex

RNA *in situ* hybridization for cortical layer markers (Reelin, Tbr1, Otx1, Er81, and SG10) in both the E18.5 Atrx^{null} and wildtype cortex indicate a loss of Er81 positive neurons of layer V in both the rostral **(A)** and caudal **(B)** sections of the Atrx^{null} cortex. Tbr1 expression also appears to be less ordered in the caudal portion of the forebrain. Loss of Er81+ neurons is associated with compromised neuronal connections resulting in difficulty translating sensory stimuli into movement.

study was initiated. It is unknown whether the DNA damage present in the Atrx^{null} cortex is due to an increase in exogenous DNA damaging agents, such as increased oxidative stress, or whether the damage observed is an accumulation of endogenous damage associated with normal differentiation. If the latter is the case, it is possible that DSBs cannot be repaired without functional Atrx. Since PARP-1 is involved in DNA repair, we hoped to inhibit its activity *in vivo* and monitor the amount of cell death with the ablation of both Atrx and Parp-1 activity.

Previous work in cell lines and mice has shown that PJ34 is a potent Parp-1 inhibitor. However, no studies have utilized this reagent on embryos via injection into pregnant mice. Here, we tested different treatment regimens to determine if we could reduce Parp-1 activity. Pregnant mice were injected with PJ34 at a dose of 1 mg/kg or 5 mg/kg at E9.5, 10.5 or both E10.5 and E12.5 prior to harvesting pups at E13.5. Figure 17 is a representative Western blot demonstrating that we were unable to sufficiently reduce Parp-1 activity. While 5 mg/kg was 5-fold higher than the dosage necessary to acquire Parp-1 inhibition in *in vivo* inflammation studies (Mabley et al., 2001), it remained insufficient to inhibit Parp-1 activity when injected peritoneally into pregnant dams. The ideal dosage regimen to achieve Parp-1 inhibition therefore remains to be elucidated.

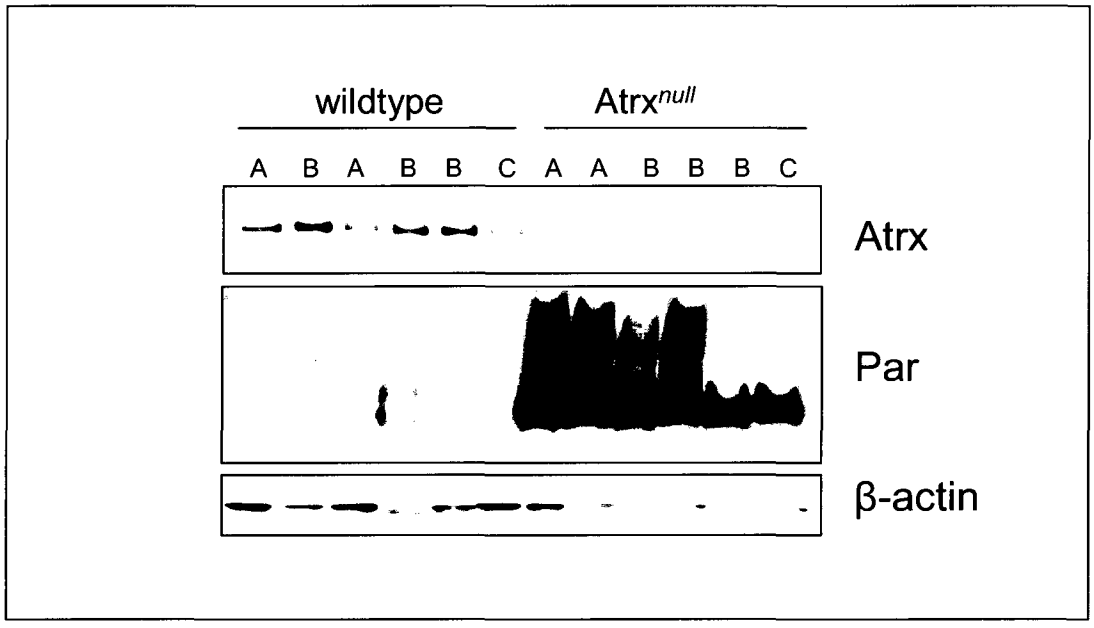

Figure 17: Parp-1 inhibitor study of E13.5 Atrx^{null} and wildtype cortical protein
Western blot analysis was performed to monitor levels of Parp-1 activity in both the Atrx^{null} and wildtype E13.5 cortex after the Parp-1 inhibitor PJ34 were administered via i.p. injection into a pregnant dam. Atrx and Par status were both verified and β-actin was used as a loading control. Parp-1 activity was not inhibited by any of the dosages tested. 10 μg of protein was loaded in each lane. Lanes are marked with a letter corresponding to the treatment received by the dam that carried the embryo. *A*: no treatment, *B*: 4 mg/kg @ E10.5, *C*: 1 mg/kg @ E10.5 and E12.5. Other dosages tested were: *D*: 1 mg/kg @ E9.5, *E*: 5 mg/kg @ E9.5. ($n_{A\text{-}wt}$=4, $n_{A\text{-}ko}$=4; $n_{B\text{-}wt}$=3, $n_{B\text{-}ko}$=3; $n_{C\text{-}wt}$=1, $n_{C\text{-}ko}$=1; $n_{D\text{-}wt}$=3, $n_{D\text{-}ko}$=3; $n_{E\text{-}wt}$=2, $n_{E\text{-}ko}$=1).

4.0 Discussion

4.1 Parp-1 in cortical development

There is currently very little information available regarding the role of Parp-1 in the cortex throughout development. Through Western blot and IHC time course experiments, levels of Parp-1 and Par were monitored throughout embryonic development to assess potential trends in Parp-1 expression and activity. Parp-1 expression appears to be slightly increased during earlier stages of corticogenesis, which is consistent with the *in vitro* N1E115 and neurosphere differentiation time courses. Additionally, monitoring of Par verified that there is increased Parp-1 activity during early stages of murine cortical development, as evidenced by large smears visible by Western blot, centering at slightly larger than 100 kDa. This is indicative of a large amount of automodified Parp-1, which is the main target of its own enzymatic activity. Parp-1 activity is barely visible from E15.5-P0.5 (Figure 10, wildtype lanes). Analysis of Par staining on brain sections shows that at E13.5, 46.8 % $\pm$ 6.2% of cells show obvious Par staining (Figure 11, wildtype). This is consistent with Western blot, as E13.5 is an embryonic time point that shows a large smear. By E17.5, no staining is visible.

Since Parp-1 is a protein that is involved in so many cellular processes, it is no surprise that there should be such a large amount of activity during the development of such a critical and complex part of the body. Parp-1 is involved in chromatin remodeling, transcription, DNA replication, apoptosis, the inflammatory response, and DNA damage and repair. Most of these processes involve its activation and most are part of normal development. For example, chromatin remodeling is a putative process of

embryonic development, as certain subsets of genes need to be activated at defined times to prompt the differentiation of a particular type of cell. The role of Parp-1 in chromatin remodeling has been reviewed in Section 1.8.1. It is thus fathomable that Parp-1 activation is occurring at early time points in corticogenesis when various neural progenitors require the proper genetic cues to differentiate. PARP-1 is also associated with DNA replication, as studies have shown that its enzymatic activity initiates DNA synthesis in cell types including hepatocytes (Cesarone et al., 1990), fibroblasts (Stone and Shall, 1975), and lymphocytes (Lehmann et al., 1974). It is entirely possible that Parp-1 activity is also required for replication in cortical development, as there is currently no evidence to the contrary.

4.2 Neurospheres

In order to more efficiently study many aspects of ATR-X syndrome, primary neurosphere cultures were characterized with the hope of developing an *in vitro* model. However, the characterization of Parp-1 activity did not recapitulate what was seen *in vivo* (Figure 13).

Although neurospheres are a valuable *in vitro* tool in many situations (Shafey et al., 2008; Hitoshi et al., 2002; Klein et al., 2005; Heins et al., 2002), the limitations of this model are highlighted in a 2006 review discussing the physiological relevance of neurospheres as a developmental model (Jensen and Parmar, 2006). Differences between our *in vivo* results and the neurosphere cultures may result from the reduction of cell-to-cell communication or the presence of certain components in the neurosphere media that influences Parp-1 activity. Additionally, a general concern regarding the neurosphere

system stems from the fact that neurospheres are a heterogeneous population containing cells that may be at different stages of differentiation, including true neural stem cells, progenitor cells, and neurons and glia that have already exited the cell cycle (Jensen and Parmar, 2006; Parmar et al., 2003; Suslov et al., 2002). In conclusion, the neurosphere system is seemingly in a very fine balance, with any slight alteration having the potential to tip the scales and result in a futile model for the study of neural development. It does not appear that the model is useful in studying the role of Parp-1 in ATR-X syndrome. However, an *in vitro* model is still desirable, and potentially promising models include siRNA knockdown of ATRX in neuronal cell lines and primary cortical neuron cultures.

4.3 Parp-1 in the Atrx^{null} cortex

With the knowledge of the baseline levels of cortical Parp-1 protein levels and activation, the subsequent matter to explore was how Parp-1 was affected when Atrx was ablated. When driving the expression of Cre recombinase under the control of the Foxg1 promoter, a conditional forebrain knockout of Atrx is generated in one quarter of the offspring of Atrx$^{f/f}$ females mated with Foxg1cre$^{+/-}$ males. Through Western blot and IHC time course experiments, levels of Parp-1 and Par were monitored throughout embryonic development in the Atrx^{null} cortex. As with wildtype mice, Parp-1 expression is increased during earlier stages of corticogenesis (Figure 10). There is no visible difference in Parp-1 expression in the Atrx^{null} cortex as compared to their wildtype littermates, suggesting that the presence of functional Atrx is not necessary for normal transcription or translation of Parp-1.

However, a large difference in Parp-1 activity was noted in the Atrx^{null} cortex

(Figure 10). While the wildtype trend of increased activity occurring at early stages of development was sustained when Atrx was lacking, the activity was largely amplified in its absence. Additionally, Par expression persists through embryonic development in the $Atrx^{null}$ forebrain when it has already been attenuated in wildtypes. The increased Par levels were not a result of Cre inclusion in these cells as Par levels were not increased in female heterozygous mice (data not shown). Quantification of IHC at E13.5 shows a significant difference between genotypes, with approximately 14% more Par^{+} cells in the $Atrx^{null}$ cortex compared to wildtype littermates (Figure 11). By E17.5, Par^{+} cells are almost completely absent when monitored by IHC, with only a very diffuse staining present in a small portion of cells (Figure 12). This is consistent with what is seen by Western blot, as only a weak Par signal is detected. This implies that the weak signal results from a small amount of activation in many cells rather than a small number of cells exhibiting a large amount of activity. These experiments suggest that Parp-1 activity is increased in the absence of Atrx, and this increase could result either directly or indirectly from the absence of Atrx.

With this finding in mind, the next logical step was to determine the cause of increased Parp-1 activity in the $Atrx^{null}$ cortex. In researching the cellular functions of Parp-1 in conjunction with what is already known about Atrx, it was decided that the two most likely possibilities were: (1) Parp-1 has a role in the previously characterized enhanced apoptotic death (Bérubé et al., 2005) ; or (2) Parp-1 is being activated as part of cell survival cascade in response to DNA damage.

To address the first possibility, the role of Parp-1 in apoptosis needed to be examined. Parp-1 is commonly involved in apoptosis in two capacities. Firstly, Parp-1 is

cleaved by caspase 3 in caspase-dependent apoptosis to prevent its overactivation and the ensuing depletion of the cell's energy pools (Kauffmann et al., 1993; Casiano et al. 1996). Secondly, the activation and subsequent automodification of Parp-1 signals for the translocation of Apoptosis Inducing Factor (AIF) from the mitochondria to the nucleus to induce a caspase-independent form of apoptosis (reviewed by Yu et al., 2002). Since cleavage of Parp-1 was not seen by Western blot (Figure 10) the status of AIF in the $Atrx^{null}$ cortex needed to be inspected. This was done by cellular fractionation and subsequent Western blot experiments with wildtype and $Atrx^{null}$ protein extracts. Antibodies for AIF show no expression changes or translocation to the nucleus, indicating that it is not detectably involved in the $Atrx^{null}$ phenotype (Figure 13). This lack of involvement of AIF suggests that the observed apoptosis is caspase-dependent, which has since been confirmed by fluorometric caspase assays. Specifically, caspase 3 activity assays (measured in arbitrary fluorescent units [a.f.u.]) showed a significant increase in E12.5 $Atrx^{null}$ cortices as compared to E12.5 wildtype cortices (8.4 ± 1.3 a.f.u. versus 2.3 ± 0.04 a.f.u, $p \leq 0.01$) (E. Goodall, unpublished). The nuclear protein p53 was also examined in this fractionation experiment, and its expression was constant throughout development in both wildtype and $Atrx^{null}$ cortical protein. This is somewhat surprising because while p53 is normally rapidly degraded in the cell, upon activation it is stabilized and accumulates in the nucleus (Jacobs et al., 2006). Since p53 has been implicated in the apoptotic pathway in the $Atrx^{null}$ cortex (Seah et al., 2008), stabilization would be expected at the early stages of corticogenesis. It is possible that it is not being activated in a large enough portion of cells to be detectable by Western blot at E13.5. A better time point to look at might be E11.5, when it was shown that there is a larger fold

increase in apoptosis (Bérubé et al., 2005). One unexpected result of this experiment arose when Atrx was shown to be present in the cytoplasm of E17.5 samples. This has been observed sporadically in some tissue staining but the reason for this finding is unknown. Interestingly, Daxx is a protein that is also predominantly nuclear but has been shown to translocate to the cytoplasm. The reason for this irregular movement is controversial, though some studies indicate it occurs in response to certain combinations of stress elements (Lindsay et al., 2009).

The second possibility addresses the fact that PARP-1 is best known as a cellular player in response to DNA damage. In order to determine if there is increased DNA damage in the $Atrx^{null}$ cortex, phosphorylated H2AX (γH2AX) was monitored. H2AX is a variant of H2A that comprises between 2 and 25% of the H2A pool. In the vicinity of double stranded breaks (DSBs), H2AX is rapidly phosphorylated at serine residue 139 by ataxia telangiectasia/Rad3-related (ATR), forming distinct foci that can be viewed by immunofluorescence (Rogakou et al., 1998). This makes γH2AX an excellent marker for DSBs in mammalian cells. It is also important to note that γH2AX is not exclusively present at DSBs, as ATR can also be activated in a cascade that recognizes single stranded breaks (SSBs) that arise at stalled replication forks and after repair of bulky DNA lesions (Chanoux et al., 2009; Pandita and Richardson, 2009; Paulsen and Cimprich, 2007).

When γH2AX was investigated, Western blot analysis showed increased levels in the $Atrx^{null}$ cortex compared to wildtype during early stages of corticogenesis. γH2AX is absent in both genotypes at more perinatal time points (Figure 15a). IHC for γH2AX at

E13.5 confirms this increase and also shows that the majority of γH2AX^{+} cells are located in the progenitor region of the cortex; again consistent with Par localization (Figure 15b). Initial quantification shows an approximate 3-fold increase in cells with γH2AX foci in the Atrx^{null} cortex as compared to wildtypes. In conclusion, since the time points exhibiting γH2AX foci correspond to those where there is an increase in Parp-1 activity, and since the location of both the foci and Parp-1 activity is heightened in the progenitor region of the cortex, these experiments provide strong evidence that Parp-1 is activated in response to DNA damage. Additionally, since DNA damage is known to be an initiator of p53-induced apoptosis, this finding fits in well with previously completed macrophage studies in our lab that show a rescue of apoptosis in Atrx^{null}p53^{null} cultures (E. Goodall, unpublished) as well as a recently published study that comes to the same conclusion *in vivo* (Seah et al., 2008).

4.4 ATRX and DNA damage and repair

While DNA is considered to be a fairly stable structure, it is actually quite susceptible to damage. This damage can occur either by endogenous or exogenous mechanisms. Even under normal physiologic conditions, nitrogenous bases can be either lost or mutated, creating abasic sites (Kunkel, 1999). Further endogenous damage can occur during replication or by DNA damaging agents that are intrinsically present in cells. Exogenous DNA damage can occur from a variety of stimuli including ultraviolet (UV) light, ionizing radiation, and genotoxic drugs (Altieri et al., 2008; Cann, K.L., and Hicks, G.G., 2007; Hegde, M.L. et al., 2008). The cause of the excess damage in the Atrx^{null} cortex is currently unknown.

When a cell is exposed to DNA damage, it will ultimately do one of two things: die, or repair itself. Although cell death by apoptosis has been shown to be occurring in the Atrx^{null} forebrain, the caspase-dependent apoptotic phenotype is not overwhelming. For instance, while caspase 3 assays performed in the lab show a significant increase in apoptosis in the Atrx^{null} cortex as compared to wildtypes, the assay still did not show a huge amount of overall activation compared to the positive control. Specifically, the positive control yielded an activity reading that was more than 5-fold higher than the Atrx^{null} samples (43.2 vs. 8.42), suggesting that the caspase activity detected is relatively weak (E. Goodall, unpublished). Additionally, while PARP-1 is typically cleaved by caspase 3 during apoptosis, we see no cleavage but rather its increased activation. Together, these seeming conflicting results indicate that while apoptosis is increased in the absence of Atrx, there is much more of this story to be elucidated.

In contemplating these results, it became necessary to consider the other possible fate of a damaged cell; the intriguing possibility that Atrx might normally be a player in DNA repair. Chromatin remodelers are commonly necessary to provide access of repair proteins to the broken DNA, and roles for other ATP-dependent chromatin remodelers in DNA repair have already been implicated in various repair pathways (reviewed by Osley et al., 2007). In particular, one recent study using human embryonic kidney (HEK) 293T cells implicates mammalian SWI/SNF chromatin remodeling complexes as having a role in contributing to cell survival, as knockdown of the catalytic subunit *BRG1* resulted in cells that were highly susceptible to DNA-damage-induced apoptosis (Park et al. 2009). In considering the findings of these studies alongside our personal observations of the Atrx^{null} phenotype, it is entirely possible that ATRX functions in a chromatin remodeling

complex that works to repair DSBs before the cell is committed to death.

There are 2 major pathways of DSB repair: Homologous recombination (HR) and non-homologous end-joining (NHEJ). The main players of the HR pathway are shown in Figure 18a. Repair of damage by HR is dependent on the stage of the cell cycle, as the sister chromosome must be in the proximity of the break to provide a template for repair.

Because of the presence of this template, HR has more potential to be error-free (Szostak et al., 1983). In contrast, NHEJ is an error prone form of repair that essentially primes the broken ends of DNA and then forces them to reconnect with the aid of a ligase enzyme. In recent years, it has been shown that there are actually two pathways that lead to the repair of DSB by NHEJ (Figure 18b-c). The main pathway is termed D-NHEJ due to its dependence on the presence of the protein DNA-PKcs. Other players include Ku70/80, Ligase IV and XRCC4. In brief, Ku70/80 recognizes the broken DNA ends and binds to them. It eventually recruits DNA-PKcs which binds the DNA, becomes activated, and phosphorylates itself and other proteins. DNA-PKcs then releases from the DNA and a Ligase IV-containing complex works to religate the broken ends with the help of a DNA polymerase (reviewed in Kinner et al., 2008). When any portion of this pathway is compromised, an alternate pathway, deemed the backup-NHEJ (B-NHEJ) pathway, takes over the repair duties (Iliakis et al., 2004; Perrault et al., 2004). The B-NHEJ pathway utilizes a repair complex that includes H1, PARP-1, and XRCC1. In this pathway, PARP-1 serves to recognize and bind to breaks. Its automodification recruits a complex containing Ligase III which works to mend the break. This discovery was quite interesting, because while this particular complex was commonly known to be involved in the repair of SSBs, it was not thought to participate in DSB repair in any capacity.

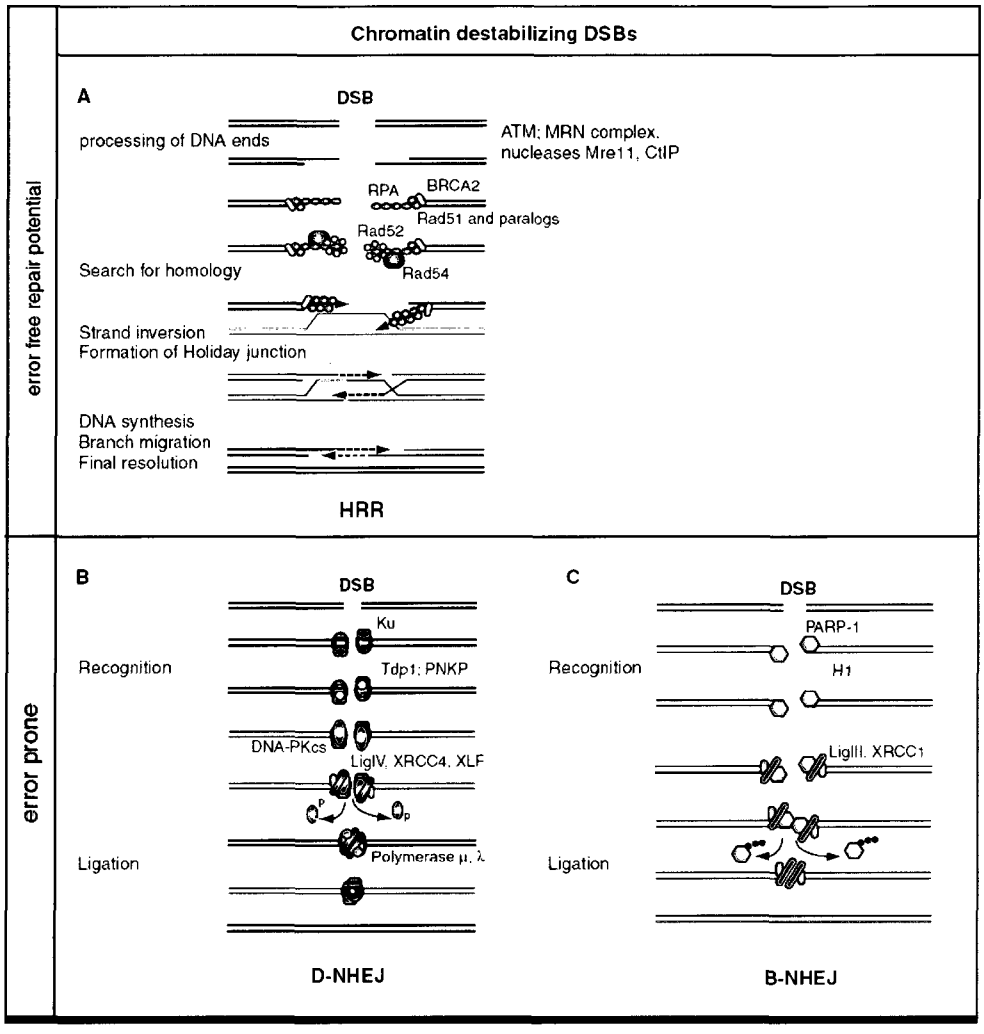

Figure 18: Double strand break repair pathways

(A) *Homologous recombination repair (HRR).* MRN senses the DSB and activates ATM which in turn phosphorylates H2AX. This initiates a signaling cascade that eventually results in nucleases (including Mre11 and CtIP) to process the DNA ends and generate ssDNA overhangs. ssDNA is bound by RPA and is subsequently exchanged by Rad51 and Rad51 paralogs. This exchange is facilitated by Rad52, Rad54 and BRCA2. The DNA containing Rad51 initiates strand inversion into an intact homologous DNA strand that then forms a Holiday junction. The sequence around the break is copied by DNA synthesis and the Holiday junction is resolved to result in repaired DNA. **(B)** *DNA-PK-dependent nonhomologous end joining (D-NHEJ).* Ku70/80 recognizes the broken DNA ends and binds to them. After processing by Tdp1 or PNKP it recruits DNA-PKcs, which then binds the DNA, activates, and phosphorylates itself and other proteins. DNA-PKcs then releases from the DNA and a Ligase IV/XRCC4/XLF complex works to religate the broken ends with the help of a DNA polymerase. **(C)** *Back up pathway of nonhomologous end joining (B-NHEJ).* The B-NHEJ takes over when a component of the D-NHEJ pathway is compromised. In this pathway, PARP-1 serves to recognize and bind to DNA ends. Modification of PARP-1 recruits a complex containing Ligase III and XRCC1 which works to mend the break. Details of this pathway remain to be elucidated, but its function is facilitated by the linker histone H1. Figure taken from Kinner et al., 2008.

However, research within the last five years regarding the B-NHEJ system has proven that this group of proteins is more active than was once believed. Mechanisms of DSB repair repair are reviewed by Pardo et al., 2009.

In hypothesizing how Atrx might fit into these repair pathways, an area that is particularly stimulating in relation to the Atrx^{null} phenotype is the two NHEJ pathways, as PARP-1 activation has a prominent role in B-NHEJ. If the normal D-NHEJ path is defective, the B-NHEJ pathway takes over to repair damage. While it is widely accepted that chromatin remodeling is a necessary step in DNA repair, a specific chromatin remodeling protein and/or protein complex has not been definitively linked to the NHEJ pathways. Hypothetically, if Atrx were involved in the D-NHEJ pathway, it would stand to reason that in its absence, PARP-1 and B-NHEJ would take over after a delay. This theory would fit in with what is seen with the activity of Parp-1 in the cortex while also explaining the early detectable damage, but remaining viability, of the Atrx^{null} embryos.

In an attempt to further study DNA repair in the Atrx^{null} cortex, we examined some DNA repair proteins involved in these NHEJ pathways. Initial Western blots for Ku and XRCC1 showed no difference in protein levels, neither between wildtype and Atrx^{null} protein or even untreated and UV-treated HEK293 cells (data not shown). These preliminary results suggest that all repair proteins tested are present but are otherwise uninformative, since repair proteins most often simply move from one part of the nucleus to the site of the break in response to damage, and typically do not show changes *in vivo* by Western blot. To further explore this hypothesis, a variety of experiments could be pursued. Immunoprecipitation experiments could be performed by pulling down Atrx and looking for interactions with any of the D-NHEJ proteins, and vice versa. These

experiments could be done following the induction of various types of DNA damage. Also, Atrx and other players in the D-NHEJ pathway could be inhibited in an *in vitro* environment and the resulting phenotypes could be compared after the induction of DNA damage. Although inhibition of the other proteins would not be expected to produce an identical phenotype to that of cells lacking Atrx, the activation of Parp-1 could be monitored as well as the amount of death and general health and morphology of the cells over a defined period of time.

Although definitive proof linking ATRX and DNA repair has not yet been found, many other neurologic diseases result from the misregulation of DNA repair proteins. These are listed in Table 5 (Brooks et al., 2008). Most interestingly, mutations in the D-NHEJ protein Ligase IV result in the autosomal recessive disorder Ligase IV syndrome. Affected individuals share several phenotypic traits with ATR-X patients, including microcephaly, distinct facial features, growth retardation, and global developmental delay (Chistiakov et al., 2009; O'Driscoll et al., 2001).

4.5 Inhibition of Parp-1 in the Atrx^{null} cortex

To further understand the role of Parp-1 in the Atrx^{null} cortex, a Parp-1 inhibitor study was initiated. The inhibitor was injected into pregnant Atrx$^{f/f}$ female mice that had been successfully time mated with a Foxg1cre$^{+/-}$ male. The plan was to then assess death by a caspase 3 assay. Parp-1 inhibition has previously been studied *in vivo* in the brain using models of stroke, and these have shown that Parp-1 inhibition has a neuroprotective effect (Kauppinen et al., 2009; Dawson, 2005). Parp-1 inhibition has had excellent

Table 5: A summary of some neurologic diseases resulting from the misregulation of DNA repair proteins. Table modified from Brooks et al., 2008.

Disease	Genes	Major CNS features
Neurodegenerative diseases		
Xeroderma pigmentosum (XP) neurologic disease	XPA,C,D,F	Primary neurodegeneration in brain, spinal cord
Ataxia telangiectasia (AT)	ATM	Purkinje neuron degeneration, movement disorders
AT-like disease	MRE11	Clinically similar to late-onset AT neurologic disease
Spinocerebellar ataxia with axonal neuropathy (SCAN1)	TDP1	Cerebellar atrophy
Ataxia with oculomotor apraxia 1	APTX (Aprataxin)	Cerebellar atrophy, axonal sensorimotor neuropathy
Ataxia with oculomotor apraxia 2	SETX	Cerebellar atrophy, axonal sensorimotor neuropathy
Ataxia with oculomotor apraxia 3	Unknown	Cerebellar atrophy
Diseases of myelin and brain calcification		
Cockayne syndrome (CS)	CSA,B; XPB,D,G	De/dysmyelination, calcification, microcephaly
Cerebro-oculo-facio-skeletal (COFS) syndrome	XPD,G; CSB, ERCC1	De/dysmyelination, calcification, microcephaly
Aicardi-Goutières syndrome (AGS)	TREX1, RNASEH2	De/dysmyelination, calcification, microcephaly, elevated CSF IFN-α, CSF lymphocytosis
Trichothiodystrophy (TTD)	XPD, TTDA	De/dysmyelination, microcephaly, ± calcification
Microcephaly diseases		
Nijmegen Breakage syndrome (NBS)	NBS1	Microcephaly, craniofacial abnormalities, mental retardation
LIG4 syndrome	LIG4	Microcephaly, craniofacial abnormalities, mental retardation
Seckel syndrome	ATR	Microcephaly, craniofacial abnormalities, mental retardation
Immunodeficiency with microcephaly	Cernunnos-XLF	Microcephaly, craniofacial abnormalities, mental retardation
Primary microcephaly 1	MCPH1/BRIT1	Microcephaly, mental retardation

results in studies where PJ34 was administered after the induction of stroke in rats, with treated rats having suppressed ischemia, increased formation of new neurons, and fewer deficits in spatial memory and learning compared to rats that did not receive PJ34 treatment (Kauppinen et al., 2009). Since Parp-1 activation is mostly associated with excessive inflammation in stroke, its inhibition results in fairly immediate positive effects. While Parp-1 inhibition has not previously been pursued in a developmental model, the use of a Parp-1 inhibitor in the Atrx^{null} model was a very exciting direction to pursue, as either increased or decreased neuronal death would be very informative in solidifying the role of Parp-1 activation upon the ablation of Atrx.

Unfortunately, although four different dosages were administered, Western blots assessing Parp-1 activity show that there is still increased activation (Figure 17). The transient effects of the inhibitor and the fact that the onset of increased Parp-1 activation is likely very early in development make it very difficult to optimize the correct dosage regimen. Additionally, Parp-1 inhibitors have not been used in pregnant mice before, and so the placenta is an extra obstacle in addition to the blood-brain barrier that the injected inhibitor needs to overcome before reaching the brain. Because of these obstacles, it is possible that to achieve sustained Parp-1 inhibition in the Atrx^{null} cortex, a higher concentration of the inhibitor needs to be injected very early in corticogenesis, with frequent subsequent injections until the desired day of harvest.

While it appears that achieving the cessation of Parp-1 activity via the injection of an inhibitor may be tedious, the goal of this experiment can theoretically still be met in another way—the development of an Atrx/Parp-1 double knockout mouse. The Parp-1 knockout mouse is viable but has impaired DNA damage repair (Wang et al., 1995;

Ménissier-de Murcia et al., 1997; Masutani et al., 1999). It is hypothesized that this enduring viability results from other Parp family members compensating for the loss of their most active member. If both Atrx and Parp-1 are ablated, it would be interesting to see how cortical development is affected. We hypothesize that if Atrx plays a role in DNA repair, the ablation of Parp-1 will result in increased cell death. The loss of Atrx will already require the initiation of an alternate system of repair, and by removing an additional repair protein in Parp-1, we would predict that cell death would be enhanced.

4.6 Loss of Er81+ neurons

Since the Atrx^{null} cortex has both cell death and DNA damage occurring early in corticogenesis, a molecular marker study was performed in E18.5 Atrx^{null} forebrains to determine if a particular cortical layer abnormality was present. E18.5 was selected as a time point in order to ensure that the cortical layers were in their proper relative positions. An embryonic time point was chosen for harvesting the samples to prevent the perinatal loss of pups that is common with this transgenic mouse line. Once the tissue was processed, IHC and *in situ* hybridization studies were performed on coronal sections. These experiments revealed that the only detectable layer abnormality in the Atrx^{null} cortex was found in layer V, where a subpopulation of Er81-expressing neurons was reduced. The presence of Otx1, a transcription factor present in the Er81^{-} subpopulation of layer V neurons, suggests that layer V neurons are not completely ablated but that the deficit is specific to those expressing Er81.

The loss of Er81^{+} neurons likely has a big impact on the Atrx^{null} phenotype. Er81 is a transcription factor of the ETS family and it marks a subpopulation of layer V

pyramidal (excitatory) neurons (De Launoit et al., 1997; Xu et al., 2000; Yoneshima et al., 2006). $Er81^+$ neurons are born between ~E12.5-E15.5, and Er81 expression is found in nearly all of the layer V neurons projecting to the spinal cord (SpC) or to the superior colliculus (SC) (Yoneshima et al., 2006). The SC is a layered structure found in the midbrain. The superficial layers of the SC receive direct visual input and the deeper, pre-motor layers receive input from the superficial layers (i.e. visual stimuli) as well as somatosensory and auditory sources. In brief, the superior colliculus is an area of convergence for many types of sensory input and it is involved in organizing and facilitating a motor response to these stimuli. It is well-characterized as having a role in gaze movement (May, 2005).

As a result of the involvement of $Er81^+$ neurons in intricate brain connections, Er81 mutant mice have severely affected motor coordination. This results from a failure of afferent neurons to form proper projections (Arber et al., 2000). Additionally, pacinian corpuscles[1] do not form in the Er81 knockout mouse (Šedý et al., 2006), and muscle spindles[2] either do not form completely or degenernate after birth (Arber et al., 2000; Kucera et al., 2002). In summary, when $Er81^+$ neurons are not present, the necessary neuronal connections to translate sensory stimuli into movement are severely compromised.

Although perinatal lethality makes it difficult to assess in depth the motor phenotype in the $Atrx^{null}$ mice, it is possible that the loss of $Er81^+$ neurons is an indirect

---

[1] mechanoreceptors that sense deep pressure

[2] sensory organs that sense muscle stretch

cause of their early death. These pups are known to be unable to obtain milk from their mothers, ultimately leading to their demise. It is possible that the loss of $Er81^{+}$ neurons results in the inability for the $Atrx^{null}$ forebrain to properly organize the necessary motor response to suckle, eventually resulting in death of the pups by dehydration (Figure 5c).

Although there is no known human syndrome associated with Er81, there are obvious similarities between the Er81 knockout mouse phenotype and that of the human ATR-X syndrome. Individuals with the ATR-X syndrome exhibit psychomotor retardation, with general hypotonia being common from early childhood. Motor milestones including sitting and walking are most often delayed, with the most severely affected individuals never being able to ambulate (Gibbons, 2006). Since Er81+ neurons play such an important role in coordinating movement, an overall impairment in motor skills would be expected in their absence.

4.7 Conclusion

In conclusion, this is the first report which links the ablation of Atrx with increased DNA damage. This finding supports previous work that links the observed apoptosis (Berube et al. 2005) with the p53 apoptotic pathway (Seah et al. 2008; Picketts unpublished), which is known to be stimulated by breaks in DNA.

Using cortical protein time courses, we were able to demonstrate that Parp-1 activity is elevated during early corticogenesis and that this elevation is further amplified in the absence of Atrx. Fractionation experiments of $Atrx^{null}$ cortical protein monitoring the cellular location of AIF do not implicate a strong role for Parp-1 activation in a caspase-independent apoptotic cascade, and instead this increase in Parp-1 activity is

likely occurring in response to an increase in DNA damage during development. This evidence suggests that the observed increase in Parp-1 activity is working to promote the survival of neurons in the $Atrx^{null}$ cortex.

Additionally, we found that there is a severe loss of layer V Er81+ cortical neurons when Atrx is ablated. These neurons are strongly associated with the coordination of movement, and so their loss could contribute to both the delayed motor milestones of ATR-X patients and the inability of $Atrx^{null}$ pups to suckle. This is the first report that links the ablation of Atrx with a loss of Er81+ neurons, and in view of the possible phenotypic implications, this finding warrants further study. It would be interesting to establish whether Atrx is either directly or indirectly involved in the differentiation of this particular type of neuron, or if these neurons are simply more susceptible to DNA damage and p53-mediated apoptosis.

5.0 References

Aasland, R., A.F. Stewart, and T. Gibson. 1996. The SANT domain: A putative DNA-binding domain in the SWI-SNF and ADA complexes, the transcriptional co-repressor N-CoR and TFIIIB. *Trends Biochem.Sci.* 21:87-88.

Ahel, I., D. Ahel, T. Matsusaka, A.J. Clark, J. Pines, S.J. Boulton, and S.C. West. 2008. Poly(ADP-ribose)-binding zinc finger motifs in DNA repair/checkpoint proteins. *Nature.* 451:81-85.

Alberts, BJ, Lewis, R, and Roberts, W. *Essential Cell Biology :4th edition.* Garland Science, New York. 2004

Altieri, F., C. Grillo, M. Maceroni, and S. Chichiarelli. 2008. DNA damage and repair: From molecular mechanisms to health implications. *Antioxidants and Redox Signaling.* 10:891-937.

Amir, R.E., I.B. Van Den Veyver, M. Wan, C.Q. Tran, U. Francke, and H.Y. Zoghbi. 1999. Rett syndrome is caused by mutations in X-linked MECP2, encoding methyl- CpG-binding protein 2. *Nat.Genet.* 23:185-188.

Andrabi, S.A., S.K. No, S.-. Yu, H. Wang, D.W. Koh, M. Sasaki, J.A. Klaus, T. Otsuka, Z. Zhang, R.C. Koehler, P.D. Hurn, G.G. Poirier, V.L. Dawson, and T.M. Dawson. 2006. Poly(ADP-ribose) (PAR) polymer is a signal. *Proc. Natl. Acad. Sci. U. S. A.* 103:18308-18313.

Arber, S., D.R. Ladle, J.H. Lin, E. Frank, and T.M. Jessell. 2000. ETS gene Er81 controls the formation of functional connections between group Ia sensory afferents and motor neurons. *Cell.* 101:485-498.

Ausubel F, Kingston RE, Brent R, Moore DD, Seidman JG, Smith JA, and K Struhl. *Short Protocols in Molecular Biology. 3rd edition* .Wiley and Sons, U.S.A.1995

Badens, C., N. Martini, S. Courrier, V. DesPortes, R. Touraine, N. Levy, and P. Edery. 2006. ATRX syndrome in a girl with a heterozygous mutation in the ATRX Zn finger domain and a totally skewed X-inactivation pattern. *American Journal of Medical Genetics, Part A.* 140:2212-2215.

Badens, C., C. Lacoste, N. Philip, N. Martini, S. Courrier, F. Giuliano, A. Verloes, A. Munnich, B. Leheup, L. Burglen, S. Odent, H. Van Esch, and N. Levy. 2006. Mutations in PHD-like domain of the ATRX gene correlate with severe psychomotor impairment and severe urogenital abnormalities in patients with ATRX syndrome. *Clin. Genet.* 70:57-62.

Baker, L.A., C.D. Allis, and G.G. Wang. 2008. PHD fingers in human diseases: Disorders arising from misinterpreting epigenetic marks. *Mutat.Res.Fundam.Mol.Mech.Mutagen.* 647:3-12

Banting, G.S., O. Barak, T.M. Ames, A.C. Burnham, M.D. Kardel, N.S. Cooch, C.E. Davidson, R. Godbout, H.E. McDermid, and R. Shiekhattar. 2005. CECR2, a protein involved in neurulation, forms a novel chromatin remodeling complex with SNF2L. *Hum.Mol.Genet.* 14:513-524.

Barak, O., M.A. Lazzaro, N.S. Cooch, D.J. Picketts, and R. Shiekhattar. 2004. A tissue-specific, naturally occurring human SNF2L variant inactivates chromatin remodeling. *J.Biol.Chem.* 279:45130-45138.

Barak, O., M.A. Lazzaro, W.S. Lane, D.W. Speicher, D.J. Picketts, and R. Shiekhattar. 2003. Isolation of human NURF: A regulator of Engrailed gene expression. *EMBO J.* 22:6089-6100.

Baumann, C., and R. De La Fuente. 2009. ATRX marks the inactive X chromosome (Xi) in somatic cells and during imprinted X chromosome inactivation in trophoblast stem cells. *Chromosoma.* 118:209-222.

Bérubé, N.G., M. Jagla, C. Smeenk, Y. De Repentigny, R. Kothary, and D.J. Picketts. 2002. Neurodevelopmental defects resulting from ATRX overexpression in transgenic mice. *Hum.Mol.Genet.* 11:253-261.

Bérubé, N.G., M. Mangelsdorf, M. Jagla, J. Vanderluit, D. Garrick, R.J. Gibbons, D.R. Higgs, R.S. Slack, and D.J. Picketts. 2005. The chromatin-remodeling protein ATRX is critical for neuronal survival during corticogenesis. *J.Clin.Invest.* 115:258-267.

Bérubé, N.G., C.A. Smeenk, and D.J. Picketts. 2000. Cell cycle-dependent phosphorylation of the ATRX protein correlates with changes in nuclear matrix and chromatin association. *Hum.Mol.Genet.* 9:539-547.

Berger, N.A. 1985. Poly(ADP-ribose) in the cellular response to DNA damage. *Radiat.Res.* 101:4-15.

Bienz, M. 2006. The PHD finger, a nuclear protein-interaction domain. *Trends Biochem.Sci.* 31:35-40.

Betz, B.L., M.W. Strobeck, D.N. Reisman, E.S. Knudsen, and B.E. Weissman. 2002. Re-expression of hSNF5/INI1/BAF47 in pediatric tumor cells leads to G1 arrest associated with induction of p16ink4a and activation of RB. *Oncogene.* 21:5193-5203.

Boerkoel, C.F., H. Takashima, J. John, J. Yan, P. Stankiewicz, L. Rosenbarker, J.-.

André, R. Bogdanovic, A. Burguet, S. Cockfield, I. Cordeiro, S. Fründ, F. Illies, M. Joseph, I. Kaitila, G. Lama, C. Loirat, D.R. McLeod, D.V. Milford, E.M. Petty, F. Rodrigo, J.M. Saraiva, B. Schmidt, G.C. Smith, J. Spranger, A. Stein, H. Thiele, J. Tizard, R. Weksberg, J.R. Lupski, and D.W. Stockton. 2002. Mutant chromatin remodeling protein SMARCAL1 causes Schimke immuno-osseous dysplasia. *Nat.Genet.* 30:215-220.

Bradford, MM. 1976. A rapid and sensitive method for the quantitation of microgram quantities of protein utilizing the principle of protein-dye binding. *Analytical Biochemistry.* 72:248-54

Brooks, P.J., T.-. Cheng, and L. Cooper. 2008. Do all of the neurologic diseases in patients with DNA repair gene mutations result from the accumulation of DNA damage? *DNA Repair.* 7:834-848.

Bultman, S., T. Gebuhr, D. Yee, C. La Mantia, J. Nicholson, A. Gilliam, F. Randazzo, D. Metzger, P. Chambon, G. Crabtree, and T. Magnuson. 2000. A Brg1 null mutation in the mouse reveals functional differences among mammalian SWI/SNF complexes. *Mol.Cell.* 6:1287-1295.

Cann, K.L., and G.G. Hicks. 2007. Regulation of the cellular DNA double-strand break response. *Biochemistry and Cell Biology.* 85:663-674.

Carson, D.A., S. Seto, D.B. Wasson, and C.J. Carrera. 1986. DNA strand breaks, NAD metabolism, and programmed cell death. *Exp.Cell Res.* 164:273-281.

Casiano, C. A., Martin, S. J., Green, D. R. and Tan, E. M. 1996. Selective cleavage of nuclear autoantigens during CD95 (Fas/APO-1)-mediated T cell apoptosis. *J. Exp. Med.* 184: 765-770.

Chambon, P., J.D. Weill, and P. Mandel. 1963. Nicotinamide mononucleotide activation of a new DNA-dependent polyadenylic acid synthesizing nuclear enzyme. *Biochem.Biophys.Res.Commun.* 11:39-43.

Chanoux, R.A., B. Yin, K.A. Urtishak, A. Asare, C.H. Bassing, and E.J. Brown. 2009. ATR and H2AX cooperate in maintaining genome stability under replication stress. *J.Biol.Chem.* 284:5994-6003.

Chiarugi, A. 2002. Poly(ADP-ribose) polymerase: Killer or conspirator? The 'suicide hypothesis' revisited. *Trends Pharmacol.Sci.* 23:122-129.

Chistiakov, D.A., N.V. Voronova, and A.P. Chistiakov. 2009. Ligase IV syndrome. *European Journal of Medical Genetics.*

Chiurazzi, P., C.E. Schwartz, J. Gecz, and G. Neri. 2008. XLMR genes: Update 2007.

European Journal of Human Genetics. 16:422-434.

Corona, D.F.V., and J.W. Tamkun. 2004. Multiple roles for ISWI in transcription, chromosome organization and DNA replication. *Biochimica Et Biophysica Acta - Gene Structure and Expression.* 1677:113-119.

D'Amours, D., S. Desnoyers, I. D'Silva, and G.G. Poirier. 1999. Poly(ADP-ribosyl)ation reactions in the regulation of nuclear functions. *Biochem.J.* 342:249-268.

Dawson, V.L. 2005. Inhibition of poly(adenosine diphosphate-ribose) polymerase (PARP) in experimental models of neurologic diseases: Cell death prevention. *Retina.* 25.

De La Fuente, R., M.M. Viveiros, K. Wigglesworth, and J.J. Eppig. 2004. ATRX, a member of the SNF2 family of helicase/ATPases, is required for chromosome alignment and meiotic spindle organization in metaphase II stage mouse oocytes. *Dev. Biol.* 272:1-14.

De Launoit, Y., J.-. Baert, A. Chotteau, D. Monte, P.-. Defossez, L. Coutte, H. Pelczar, and F. Leenders. 1997. Structure-function relationships of the PEA3 group of Ets-related transcription factors. *Biochem.Mol.Med.* 61:127-135.

Deuring, R., L. Fanti, J.A. Armstrong, M. Sarte, O. Papoulas, M. Prestel, G. Daubresse, M. Verardo, S.L. Moseley, M. Berloco, T. Tsukiyama, C. Wu, S. Pimpinelli, and J.W. Tamkun. 2000. The ISWI chromatin-remodeling protein is required for gene expression and the maintenance of higher order chromatin structure in vivo. *Mol.Cell.* 5:355-365.

Diaz-Hernandez, J.I., S. Moncada, J.P. Bolaños, and A. Almeida. 2007. Poly(ADP-ribose) polymerase-1 protects neurons against apoptosis induced by oxidative stress. *Cell Death Differ.* 14:1211-1221.

Ehrlich, M., M.A. Gama-Sosa, L.H. Huang, R.M. Midgett, K.C. Kuo, R.A. McCune, and C. Gehrke. 1982. Amount and distribution of 5-methylcytosine in human DNA from different types of tissues of cells. *Nucleic Acids Res.* 10:2709-2721.

Fan, G., C. Beard, R.Z. Chen, G. Csankovszki, Y. Sun, M. Siniaia, D. Biniszkiewicz, B. Bates, P.P. Lee, R. Ku□hn, A. Trumpp, C.-. Poon, C.B. Wilson, and R. Jaenisch. 2001. DNA hypomethylation perturbs the function and survival of CNS neurons in postnatal animals. *Journal of Neuroscience.* 21:788-797.

Fernandez-Capetillo, O., A. Lee, M. Nussenzweig, and A. Nussenzweig. 2004. H2AX: The histone guardian of the genome. *DNA Repair.* 3:959-967.

Garrick, D., V. Samara, T.L. McDowell, A.J.H. Smith, L. Dobbie, D.R. Higgs, and R.J. Gibbons. 2004. A conserved truncated isoform of the ATR-X syndrome protein lacking the SWI/SNF-homology domain. *Gene.* 326:23-34.

Garrick, D., J.A. Sharpe, R. Arkell, L. Dobbie, A.J. Smith, W.G. Wood, D.R. Higgs, and R.J. Gibbons. 2006. Loss of Atrx affects trophoblast development and the pattern of X-inactivation in extraembryonic tissues. *PLoS Genetics.* 2.

Gayther, S.A., S.J. Batley, L. Linger, A. Bannister, K. Thorpe, S.-. Chin, Y. Daigo, P. Russell, A. Wilson, H.M. Sowter, J.D.A. Delhanty, B.A.J. Ponder, T. Kouzarides, and C. Caldas. 2000. Mutations truncating the EP300 acetylase in human cancers. *Nat.Genet.* 24:300-303.

Geiman, T.M., and K.D. Robertson. 2002. Chromatin remodeling, histone modifications, and DNA methylation - How does it all fit together? *J.Cell.Biochem.* 87:117-125.

Gibbons, R. 2006. Alpha thalassaemia-mental retardation, X linked. *Orphanet J. Rare Dis.* 1.

Gibbons, R.J., T.L. McDowell, S. Raman, D.M. O'Rourke, D. Garrick, H. Ayyub, and D.R. Higgs. 2000. Mutations in ATRX, encoding a SWI/SNF-like protein, cause diverse changes in the pattern of DNA methylation. *Nat.Genet.* 24:368-371.

Gibbons, R.J., T. Wada, C.A. Fisher, N. Malik, M.J. Mitson, D.P. Steensma, A. Fryer, D.R. Goudie, I.D. Krantz, and J. Traeger-Synodinos. 2008. Mutations in the chromatin-associated protein ATRX. *Hum. Mutat.* 29:796-802.

Grewal, S.I.S., and S. Jia. 2007. Heterochromatin revisited. *Nature Reviews Genetics.* 8:35-46.

Gupta, A., L.-. Tsai, and A. Wynshaw-Boris. 2002. Life is a journey: A genetic look at neocortical development. *Nature Reviews Genetics.* 3:342-355.

Haynes, S.R., C. Dollard, F. Winston, S. Beck, J. Trowsdale, and I.B. Dawid. 1992. The bromodomain: A conserved sequence found in human, Drosophila and yeast proteins. *Nucleic Acids Res.* 20:2603.

Hegde, M.L., T.K. Hazra, and S. Mitra. 2008. Early steps in the DNA base excision/single-strand interruption repair pathway in mammalian cells. *Cell Research.* 18:27-47.

Heins, N., P. Malatesta, F. Cecconi, M. Nakafuku, K.L. Tucker, M.A. Hack, P. Chapouton, Y.-. Barde, and M. Go□tz. 2002. Glial cells generate neurons: The role of the transcription factor Pax6. *Nat.Neurosci.* 5:308-315.

Hitoshi, S., V. Tropepe, M. Ekker, and D. van der Kooy. 2002. Neural stem cell lineages are regionally specified, but not committed, within distinct compartments of the developing brain. *Development.* 129:233-244.

Hsieh, J., and F.H. Gage. 2005. Chromatin remodeling in neural development and plasticity. *Curr.Opin.Cell Biol.* 17:664-671.

Huang, C., E.A. Sloan, and C.F. Boerkoel. 2003. Chromatin remodeling and human disease. *Curr.Opin.Genet.Dev.* 13:246-252.

Iliakis, G., H. Wang, A.R. Perrault, W. Boecker, B. Rosidi, F. Windhofer, W. Wu, J. Guan, G. Terzoudi, and G. Panteliasc. 2004. Mechanisms of DNA double strand break repair and chromosome aberration formation. *Cytogenetic and Genome Research.* 104:14-20.

Iizuka, M., and M.M. Smith. 2003. Functional consequences of histone modifications. *Curr.Opin.Genet.Dev.* 13:154-160.

Ion, A., L. Telvi, J.L. Chaussain, F. Galacteros, J. Valayer, M. Fellous, and K. McElreavey. 1996. A novel mutation in the putative DNA helicase XH2 is responsible for male- to-female sex reversal associated with an atypical form of the ATR-X syndrome. *Am.J.Hum.Genet.* 58:1185-1191.

Jacobs WB, Kaplan DR and FD Miller. 2006. The p53 family in nervous system development and disease. *Journal of Neurochemistry.* 97:1571-84

Jensen AM and VA Wallace. 1997. Expression of Sonic hedgehog and its putative role as a precursor cell mitogen in the developing mouse retina. *Development.* 124: 363-371.

Jensen, J.B., and M. Parmar. 2006a. Strengths and limitations of the neurosphere culture system. *Mol.Neurobiol.* 34:153-161.

Johnson, C.N., N.L. Adkins, and P. Georgel. 2005. Chromatin remodeling complexes: ATP-dependent machines in action. *Biochemistry and Cell Biology.* 83:405-417.

Kaufmann, S.H., S. Desnoyers, Y. Ottaviano, N.E. Davidson, and G.G. Poirier. 1993. Specific proteolytic cleavage of poly(ADP-ribose) polymerase: An early marker of chemotherapy-induced apoptosis. *Cancer Res.* 53:3976-3985.

Kauppinen, T.M., S.W. Suh, A.E. Berman, A.M. Hamby, and R.A. Swanson. 2009. Inhibition of poly(ADP-ribose) polymerase suppresses inflammation and promotes recovery after ischemic injury. *Journal of Cerebral Blood Flow and Metabolism.* 29:820-829.

Kidder, B.L., S. Palmer, and J.G. Knott. 2009. SWI/SNF-brg1 regulates self-renewal and occupies core pluripotency-related genes in embryonic stem cells. *Stem Cells.* 27:317-328.

Kim, M.Y., S. Mauro, N. Gévry, J.T. Lis, and W.L. Kraus. 2004. NAD+-dependent

modulation of chromatin structure and transcription by nucleosome binding properties of PARP-1. *Cell.* 119:803-814.

Klein, C., S.J.B. Butt, R.P. Machold, J.E. Johnson, and G. Fishell. 2005. Cerebellum- and forebrain-derived stem cells possess intrinsic regional character. *Development.* 132:4497-4508.

Koh, D.W., T.M. Dawson, and V.L. Dawson. 2005a. Mediation of cell death by poly(ADP-ribose) polymerase-1. *Pharmacol. Res.* 52:5-14.

Koh, D.W., T.M. Dawson, and V.L. Dawson. 2005b. Poly(ADP-ribosyl)ation regulation of life and death in the nervous system. *Cell. Mol. Life Sci.* 62:760-768.

Kraus, W.L., and J.T. Lis. 2003. PARP goes transcription. *Cell.* 113:677-683.

Kucera, J., W. Cooney, A. Que, V. Szeder, H. Stancz-Szeder, and J. Walro. 2002. Formation of supernumerary muscle spindles at the expense of Golgi tendon organs in ER81-deficient mice. *Developmental Dynamics.* 223:389-401.

Kumari, D., and K. Usdin. 2009. Chromatin remodeling in the noncoding repeat expansion diseases. *The Journal of Biological Chemistry.* 284:7413-7417.

Kung, A.L., V.I. Rebel, R.T. Bronson, L.-. Ch'ng, C.A. Sieff, D.M. Livingston, and T.-. Yao. 2000. Gene dose-dependent control of hematopoiesis and hematologic tumor suppression by CBP. *Genes and Development.* 14:272-277.

Kunkel, T.A. 1999. The high cost of living. *Trends in Genetics.* 15:93-94.

Lall, S. 2007. Primers on chromatin. *Nature Structural and Molecular Biology.* 14:1110-1115.

Lehmann, A.R., S. Kirk Bell, S. Shall, and W.J.D. Whish. 1974. The relationship between cell growth, macromolecular synthesis and poly ADP ribose polymerase in lymphoid cells. *Exp.Cell Res.* 83:63-72.

Leonard, H., and X. Wen. 2002. The epidemiology of mental retardation: Challenges and opportunities in the new millennium. *Ment.Retard.Dev.Disabil.Res.Rev.* 8:117-134.

Lessard, J., J.I. Wu, J.A. Ranish, M. Wan, M.M. Winslow, B.T. Staahl, H. Wu, R. Aebersold, I.A. Graef, and G.R. Crabtree. 2007. An Essential Switch in Subunit Composition of a Chromatin Remodeling Complex during Neural Development. *Neuron.* 55:201-215.

Lindsay, C.R., S. Giovinazzi, and A.M. Ishov. 2009. Daxx is a predominately nuclear protein that does not translocate to the cytoplasm in response to cell stress. *Cell Cycle.* 8:1544-1551.

Lisik, M.Z., and A.L. Sieron. 2008. X-linked mental retardation. *Medical Science Monitor.* 14:RA221-RA229.

Mabley, J.G., P. Jagtap, M. Perretti, S.J. Getting, A.L. Salzman, L. Virág, É. Szabó, F.G. Soriano, L. Liaudet, G.E. Abdelkarim, G. Haskó, A. Marton, G.J. Southan, and C. Szabó. 2001. Anti-inflammatory effects of a novel, potent inhibitor of poly(ADP-ribose) polymerase. *Inflammation Res.* 50:561-569.

Masutani, M., T. Nozaki, E. Nishiyama, T. Shimokawa, Y. Tachi, H. Suzuki, H. Nakagama, K. Wakabayashi, T. Sugimura. 1999. Function of poly(ADP-ribose) polymerase in response to DNA damage: Gene-disruption study in mice. *Mol. Cell. Biochem.* 193: 149-152

May, P.J. 2005. The mammalian superior colliculus: Laminar structure and connections. *Progress in Brain Research.* 151:321-378.

McDowell, T.L., R.J. Gibbons, H. Sutherland, D.M. O'Rourke, W.A. Bickmore, A. Pombo, H. Turley, K. Gatter, D.J. Picketts, V.J. Buckle, L. Chapman, D. Rhodes, and D.R. Higgs. 1999. Localization of a putative transcriptional regulator (ATRX) at pericentromeric heterochromatin and the short arms of acrocentric chromosomes. *Proc.Natl.Acad.Sci.U.S.A.* 96:13983-13988.

McPherson, E.W., M.M. Clemens, R.J. Gibbons, and D.R. Higgs. 1995. X-linked α-thalassemia/mental retardation (ATR-X) syndrome: A new kindred with severe genital anomalies and mild hematologic expression. *Am.J.Med.Genet.* 55:302-306.

Meehan, R.R., J.D. Lewis, S. McKay, E.L. Kleiner, and A.P. Bird. 1989. Identification of a mammalian protein that binds specifically to DNA containing methylated CpGs. *Cell.* 58:499-507.

Ménussier-de Murcia, J., C. Niedergang, C. Trucco, M. Ricoul, B. Dutrillaux, M. Mark, F.J. Oliver, M. Masson, A. Dierich, M. LeMeur, C. Walztinger, P. Chambon, G. de Murcia. 1997. Requirement of poly(ADP-ribose) polymerase in recovery from DNA damage in mice and in cells. *Proc. Natl. Acad. Sci. U.S.A.* 94: 7303-7307.

Murata, T., R. Kurokawa, A. Krones, K. Tatsumi, M. Ishii, T. Taki, M. Masuno, H. Ohashi, M. Yanagisawa, M.G. Rosenfeld, C.K. Glass, and Y. Hayashi. 2001. Defect of histone acetyltransferase activity of the nuclear transcriptional coactivator CBP in Rubinstein-Taybi syndrome. *Hum.Mol.Genet.* 10:1071-1076.

Nan, X., J. Hou, A. Maclean, J. Nasir, M.J. Lafuente, X. Shu, S. Kriaucionis, and A. Bird. 2007. Interaction between chromatin proteins MECP2 and ATRX is disrupted by mutations that cause inherited mental retardation. *Proc. Natl. Acad. Sci. U. S. A.* 104:2709-2714.

Narlikar, G.J., H.-. Fan, and R.E. Kingston. 2002. Cooperation between complexes that regulate chromatin structure and transcription. *Cell.* 108:475-487.

Nastase Byrd, K., and A. Shearn. 2003. ASH1, a Drosophila trithorax group protein, is required for methylation of lysine 4 residues on histone H3. *Proc.Natl.Acad.Sci.U.S.A.* 100:11535-11540.

Nusinow, D.A., I. Hernández-Mun~oz, T.G. Fazzio, G.M. Shah, W.L. Kraus, and B. Panning. 2007. Poly(ADP-ribose) polymerase 1 is inhibited by a histone H2A variant, macroH2A, and contributes to silencing of the inactive X chromosome. *J. Biol. Chem.* 282:12851-12859.

O'Driscoll, M., K.M. Cerosaletti, P.-. Girard, Y. Dai, M. Stumm, B. Kysela, B. Hirsch, A. Gennery, S.E. Palmer, J. Seidel, R.A. Gatti, R. Varon, M.A. Oettinger, H. Neitzel, P.A. Jeggo, and P. Concannon. 2001. DNA ligase IV mutations identified in patients exhibiting developmental delay and immunodeficiency. *Mol.Cell.* 8:1175-1185.

Okano, M., S. Xie, and E. Li. 1998. Cloning and characterization of a family of novel mammalian DNA (cytosine-5) methyltransferases [1]. *Nat.Genet.* 19:219-220.

Oleinick, N.L., and H.H. Evans. 1985. Poly(ADP-ribose) and the response of cells to ionizing radiation. *Radiat.Res.* 101:29-46.

Osley, M.A., T. Tsukuda, and J.A. Nickoloff. 2007. ATP-dependent chromatin remodeling factors and DNA damage repair. *Mutation Research - Fundamental and Molecular Mechanisms of Mutagenesis.* 618:65-80.

Pandita, T.K., and C. Richardson. 2009. Chromatin remodeling finds its place in the DNA double-strand break response. *Nucleic Acids Res.* 37:1363-1377.

Pardo, B., B. Gómez-González, and A. Aguilera. 2009. DNA double-strand break repair: How to fix a broken relationship. *Cellular and Molecular Life Sciences.* 66:1039-1056.

Park, J., E. Park, S. Hur, S. Kim, J. Kwon. 2009. Mammalian SWI/SNF chromatin remodeling complexes are required to prevent apoptosis after DNA damage. *DNA Repair.* 8: 29-39.

Parmar, M., C. Skogh, and U. Englund. 2003. A transplantation study of expanded human embryonic forebrain precursors: Evidence for selection of a specific progenitor population. *Molecular and Cellular Neuroscience.* 23:531-543.

Paulsen, R.D., and K.A. Cimprich. 2007. The ATR pathway: Fine-tuning the fork. *DNA Repair.* 6:953-966.

Perrault, R., H. Wang, M. Wang, B. Rosidi, and G. Iliakis. 2004. Backup pathways of NHEJ are suppressed by DNA-PK. *J.Cell.Biochem.* 92:781-794.

Peters, A.H.F.M., and D. Schübeler. 2005. Methylation of histones: Playing memory with DNA. *Curr.Opin.Cell Biol.* 17:230-238.

Quénet, D., R. El Ramy, V. Schreiber, and F. Dantzer. 2009. The role of poly(ADP-ribosyl)ation in epigenetic events. *Int.J.Biochem.Cell Biol.* 41:60-65.

Raymond, F.L. 2006. X linked mental retardation: A clinical guide. *J. Med. Genet.* 43:193-200.

Reale, A., G. De Matteis, G. Galleazzi, M. Zampieri, and P. Caiafa. 2005. Modulation of DNMT1 activity by ADP-ribose polymers. *Oncogene.* 24:13-19.

Ritchie, K., C. Seah, J. Moulin, C. Isaac, F. Dick, and N.G. Bérubé. 2008. Loss of ATRX leads to chromosome cohesion and congression defects. *J. Cell Biol.* 180:315-324.

Rogakou, E.P., D.R. Pilch, A.H. Orr, V.S. Ivanova, and W.M. Bonner. 1998. DNA double-stranded breaks induce histone H2AX phosphorylation on serine 139. *J.Biol.Chem.* 273:5858-5868.

Santos-Rosa, H., R. Schneider, A.J. Bannister, J. Sherriff, B.E. Bernstein, N.C.T. Emre, S.L. Schreiber, J. Mellor, and T. Kouzarides. 2002. Active genes are tri-methylated at K4 of histone H3. *Nature.* 419:407-411.

Saxena, A., R. Saffery, L.H. Wong, P. Kalitsis, and K.H.A. Choo. 2002a. Centromere proteins Cenpa, Cenpb, and Bub3 interact with poly(ADP-ribose) polymerase-1 protein and are poly(ADP-ribosyl)ated. *J.Biol.Chem.* 277:26921-26926.

Saxena, A., L.H. Wong, P. Kalitsis, E. Earle, L.G. Shaffer, and K.H.A. Choo. 2002b. Poly(ADP-ribose) polymerase 2 localizes to mammalian active centromeres and interacts with PARP-1, Cenpa, Cenpb and Bub3, but not Cenpc. *Hum.Mol.Genet.* 11:2319-2329.

Seah, C., M.A. Levy, Y. Jiang, S. Mokhtarzada, D.R. Higgs, R.J. Gibbons, and N.G. Bérubé. 2008. Neuronal death resulting from targeted disruption of the Snf2 protein ATRX is mediated by p53. *Journal of Neuroscience.* 28:12570-12580.

Šedý, J., S. Tseng, J.M. Walro, M. Grim, and J. Kucera. 2006. ETS transcription factor ER81 is required for the Pacinian corpuscle development. *Developmental Dynamics.* 235:1081-1089.

Shafey, D., A.E. MacKenzie, and R. Kothary. 2008. Neurodevelopmental abnormalities in neurosphere-derived neural stem cells from SMN-depleted mice. *J.Neurosci.Res.* 86:2839-2847.

Sharma, R.P., D.R. Grayson, A. Guidotti, and E. Costa. 2005. Chromatin, DNA methylation and neuron gene regulation - The purpose of the package. *J.Psychiatry Neurosci.* 30:257-263.

Shiao Li Oei, and M. Ziegler. 2000. ATP for the DNA ligation step in base excision repair is generated from poly(ADP-ribose). *J.Biol.Chem.* 275:23234-23239.

Stone, P.R., and S. Shall. 1975. Poly (ADP ribose) polymerase activity during the growth cycle of mouse fibroblasts (LS cells). *Exp.Cell Res.* 91:95-100.

Stopka, T., and A.I. Skoultchi. 2003. The ISWI ATPase Snf2h is required for early mouse development. *Proc.Natl.Acad.Sci.U.S.A.* 100:14097-14102.

Sugita, K., T. Taki, Y. Hayashi, H. Shimaoka, H. Kumazaki, H. Inoue, Y. Konno, M. Taniwaki, H. Kurosawa, and M. Eguchi. 2000. MLL-CBP fusion transcript in a therapy-related acute myeloid leukemia with the t(11;16)(q23;p13) which developed in an acute lymphoblastic leukemia patient with Fanconi anemia. *Genes Chromosomes and Cancer.* 27:264-269.

Sung Jae Lee, S., M. Wan, and U. Francke. 2001. Spectrum of MECP2 mutations in Rett syndrome. *Brain and Development.* 23:S138-S143.

Suslov, O.N., V.G. Kukekov, T.N. Ignatova, and D.A. Steindler. 2002. Neural stem cell heterogeneity demonstrated by molecular phenotyping of clonal neurospheres. *Proc.Natl.Acad.Sci.U.S.A.* 99:14506-14511.

Szostak, J.W., T.L. Orr Weaver, and R.J. Rothstein. 1983. The double-strand-break repair model for recombination. *Cell.* 33:25-35

Tang, P., D.J. Park, J.A.M. Graves, and V.R. Harley. 2004. ATRX and sex differentiation. *Trends in Endocrinology and Metabolism.* 15:339-344.

Thienpont, B., T. de Ravel, H. Van Esch, D. Van Schoubroeck, P. Moerman, J.R. Vermeesch, J.-. Fryns, G. Froyen, C. Lacoste, C. Badens, and K. Devriendt. 2007. Partial duplications of the ATRX gene cause the ATR-X syndrome. *Eur. J. Hum. Genet.* 15:1094-1097.

Truett GE, Heeger P, Mynatt RL, Truett AA, Walker JA and ML Warman. 2000. Preparation of PCR-quality mouse genomic DNA with hot sodium hydroxide and tris (HotSHOT). *Biotechniques.* 29:52-4

Tulin, A., Y. Chinenov, and A. Spradling. 2003. Regulation of Chromatin Structure and Gene Activity by Poly(ADP-Ribose) Polymerases. *Current Topics in Developmental Biology.* 56:55-83.

Tulin, A., and A. Spradling. 2003. Chromatin loosening by poly(ADP)-ribose polymerase (PARP) at Drosophila puff loci. *Science.* 299:560-562.

Tulin, A., D. Stewart, and A.C. Spradling. 2002. The Drosophila heterochromatic gene

encoding poly(ADP-ribose) polymerase (PARP) is required to modulate chromatin structure during development. *Genes and Development.* 16:2108-2119.

Van Hoffen, A., A.T. Natarajan, L.V. Mayne, A.A. Van Zeeland, L.H.F. Mullenders, and J. Venema. 1993. Deficient repair of the transcribed strand of active genes in Cockayne's syndrome cells. *Nucleic Acids Res.* 21:5890-5895.

Wada, T., M. Nakamura, Y. Matsushita, M. Yamada, S. Yamashita, H. Iwamoto, M. Masuno, K. Imaizumi, and Y. Kuroki. 1998. Three Japanese children with X-linked α-thalassemia/mental retardation syndrome (ATR-X). *No to.Hattatsu.* 30:283-289.

Wada, T., H. Sugie, Y. Fukushima, and S. Saitoh. 2005. Non-skewed X-inactivation may cause mental retardation in a female carrier of X-linked α-thalassemia/mental retardation syndrome (ATR-X): X-inactivation study of nine female carriers of ATR-X. *Am. J. Med. Genet.* 138 A:18-20.

Wang, Z.Q., B. Auer, L. Stingl, H. Berghammer, D. Haidacher, M. Schweiger, E.W. Wagner. 1995. Mice lacking ADPRT and poly(ADP-ribosyl)ation develop normally but are susceptible to skin disease. *Genes Dev.* 9: 509-520.

Winston, F., and C. David Allis. 1999. The bromodomain: A chromatin-targeting module? *Nat.Struct.Biol.* 6:601-604.

Xu, B., K. Zang, N.L. Ruff, Y.A. Zhang, S.K. McConnell, M.P. Stryker, and L.F. Reichardt. 2000. Cortical degeneration in the absence of neurotrophin signaling: Dendritic retraction and neuronal loss after removal of the receptor TrkB. *Neuron.* 26:233-245.

Xue, Y., R. Gibbons, Z. Yan, D. Yang, T.L. McDowell, S. Sechi, J. Qin, S. Zhou, D. Higgs, and W. Wang. 2003. The ATRX syndrome protein forms a chromatin-remodeling complex with Daxx and localizes in promyelocytic leukemia nuclear bodies. *Proc. Natl. Acad. Sci. U. S. A.* 100:10635-10640.

Yoneshima, H., S. Yamasaki, C.C.J. Voelker, Z. Molnár, E. Christophe, E. Audinat, M. Takemoto, M. Nishiwaki, S. Tsuji, I. Fujita, and N. Yamamoto. 2006. ER81 is expressed in a subpopulation of layer 5 neurons in rodent and primate neocortices. *Neuroscience.* 137:401-412.

Yu, S.-., H. Wang, T.M. Dawson, and V.L. Dawson. 2003. Poly(ADP-ribose) polymerase-1 and apoptosis inducing factor in neurotoxicity. *Neurobiol. Dis.* 14:303-317.

Yu, S.-., H. Wang, M.F. Poitras, C. Coombs, W.J. Bowers, H.J. Federoff, G.G. Poirier, T.M. Dawson, and V.L. Dawson. 2002. Mediation of poty(ADP-ribose) polymerase-1 - Dependent cell death by apoptosis-inducing factor. *Science.* 297:259-263.